IEEE Access
Multidisciplinary ⋮ Rapid Review ⋮ Open Access Journal

Received 2 June 2025, accepted 16 September 2025, date of publication 19 September 2025, date of current version 25 September 2025.

Digital Object Identifier 10.1109/ACCESS.2025.3612294

RESEARCH ARTICLE

Techno-Economic, Environmental, and Social Multi-Objective Optimization of a Grid-Connected Hybrid Renewable Energy System Using Metaheuristic Algorithms

DHRUTI DHEDA[1], JANDRÉ ALBERTYN[1], KAYODE ADETUNJI[1], ZHENQING LIU[2], ADNAN M. ABU-MAHFOUZ[3], (Senior Member, IEEE), AND LING CHENG[1], (Senior Member, IEEE)

[1]School of Electrical and Information Engineering, University of the Witwatersrand, Johannesburg 2000, South Africa
[2]School of Civil and Hydraulic Engineering, Huazhong University of Science and Technology, Wuhan 430074, China
[3]Council for Scientific and Industrial Research (CSIR), Pretoria 0001, South Africa

Corresponding author: Ling Cheng (Ling.Cheng@wits.ac.za)

ABSTRACT The transition from fossil fuels to renewable energy demands energy systems that are not only technically and economically sound but also environmentally and socially sustainable. This study proposed a novel multi-objective optimisation (MOO) framework for the design of a grid-connected hybrid renewable energy system (GC-HRES) that explicitly integrated Job Creation (JC) as a fourth objective along with traditional technical, economic, and environmental objectives, such as Loss of Power Supply Probability (LPSP), Cost of Energy (COE), and Renewable Energy Fraction (REF). Prior studies often treated JC as a post-optimisation metric, while this study incorporated JC into the MOO using employment technology-specific factors. Metaheuristic algorithms, Multi-Objective Particle Swarm Optimisation (MOPSO) and Non-Dominated Sorting Genetic Algorithm II (NSGA-II), were applied to find the optimal number of solar panels, wind turbines, and battery banks under scenarios which excluded and included JC. The results demonstrated that including JC reshaped the Pareto front, revealed new objective compromises and led to diverse configurations. MOPSO favoured solutions with higher JC and REF at the expense of cost and reliability, while NSGA-II achieved more balanced, cost-effective and reliable solutions with competitive JC values. Additional constraint sensitivity analysis further demonstrated the influence of battery bank constraints on solution feasibility. The results highlighted that integrating JC into the optimisation framework enriched design possibilities and fostered a more inclusive transition to renewable energy with a focus on GC-HRESs. This paper provided a flexible and replicable MOO framework that sets the foundation for socially attuned GC-HRES designs that align with broader sustainability goals.

INDEX TERMS Cost of energy, hybrid renewable energy systems, job creation, loss of power supply probability, machine learning metaheuristic algorithms, multiple objective optimization, non-dominated sorting genetic algorithm II, particle swarm optimization, renewable energy, renewable energy fraction, solar panels, wind turbines.

I. INTRODUCTION

The dependence on non-renewable fossil fuels is unsustainable and increasingly uneconomical, especially given the escalating severity of climate change. Renewable Energy Sources (RESs) offer a viable alternative by reducing reliance on fossil fuels [1], [2]. However, the inherent volatility and intermittency of RESs limit the reliability and stability of the energy they produce. To address this limitation, Hybrid Renewable Energy Systems (HRESs), which combine two

The associate editor coordinating the review of this manuscript and approving it for publication was Daniela Cristina Momete.

or more complementary RESs with backup energy sources and energy storage, have been proposed [3]. The proposition of HRESs as alternative energy systems is fundamentally connected to the environmental and social benefits of RESs and thus carries implicit social impacts.

The design of HRESs usually involves optimising the number of renewable energy components or the size of one or more of the components (for example, the wind turbine or solar panel). The objectives and preferences of the stakeholders guide which aspects of the HRES are selected for optimisation [3]. Performance and impact criteria, expressed as numerical objective functions, are used to optimise HRESs. The objective functions are either minimised or maximised in a multi-objective optimisation (MOO) design problem to identify the optimal HRES configuration. The MOO not only finds the optimal configurations that satisfies the functional requirements defined by stakeholders, but also quantifies and evaluates the performance and impact of the HRES across multiple dimensions [2].

Initially, HRES design and sizing were optimised on a techno-economic basis and benchmarked against conventional profit-driven fossil fuel systems. A review of 299 journal articles published over the past five years found that 97.99% focused primarily on economic objectives in HRES sizing optimisation. Economic objectives were frequently paired with technical objectives [3]. However, this narrow focus fails to capture the full impact of HRESs by omitting environmental and social dimensions. A truly holistic evaluation should integrate technical, economic, environmental, and social objectives into the design optimisation process [2].

HRESs offer numerous environmental and social benefits. These benefits are advantages that should be evaluated and highlighted when comparing HRESs with fossil fuel systems to assess overall feasibility [2]. To encourage large-scale adoption, HRESs must demonstrate superior feasibility in comparison to conventional energy systems. Although technical and economic performance remains essential, fully capturing the potential of HRESs requires integrating environmental and social benefits into feasibility evaluations [2].

In recent years, the MOO frameworks of HRESs have expanded to include environmental objectives. However, social objectives remain largely overlooked, even though some studies have begun to address them. Most MOO solutions do not yet comprehensively assess the social impacts of HRESs [3]. Incorporating social objectives into HRES optimisation is therefore essential for deepening our understanding in this area, stimulating further research, and developing robust, holistically efficient energy systems.

Solar and wind energy are among the most commonly deployed renewable energy sources in HRESs. However, their power output varies with environmental conditions, resulting in intermittent power generation. Integrating both solar and wind energy within grid-connected (GC)-HRESs significantly enhances the reliability and efficiency of the generated power supply [4].

This paper aims to determine the optimal design configuration of a GC-HRES using a MOO that simultaneously addresses technical, economic, environmental and social objectives to create an energy system that is technically sound, economically viable, environmentally sustainable and socially beneficial.

A study by [5] explores the MOO of a GC-HRES and addresses technical, economic, and environmental objectives using the Multi-Objective Particle Swarm optimisation (MOPSO) algorithm. The system in this case study is located in Abu Atwa Village, Ismailia Governorate, Egypt, which has abundant renewable energy potential. Firstly, this paper will replicate the three-objective MOPSO optimisation study by [5]. The paper will then extend the MOO framework by introducing a social objective as the fourth optimisation criterion.

This paper highlights the importance of including social factors in the MOO of GC-HRESs, a research area that is still relatively unexplored despite recent progress. This paper focuses specifically on the addition of social objectives to GC-HRESs rather than standalone systems. The integrated MOO framework presented in this paper simultaneously optimises one representative objective from each domain, technical, economic, environmental, and social, providing a holistic evaluation of the impact and sustainability of the GC-HRES. By selecting a single objective per domain, this paper emphasises the effects of including an additional social objective in the optimisation process and the subsequent effect on the other objectives.

This paper will retain the technical, economic and environmental objectives that were used in the study by [5]. The Loss of Power Supply Probability (LPSP) is a reliability marker and technical objective, while the Cost of Energy (COE) is the economic objective. Both LPSP and COE will be minimised in the MOO, while the environmental objective, the Renewable Energy Fraction (REF), will be maximised. All three objectives are discussed in greater detail later in this paper.

This paper selects Job Creation (JC) as the fourth objective in the MOO framework. JC was chosen for its dual benefits. JC has advantageous social impacts and is strongly related to economic gains, factors that are especially critical for developing countries in the global south [6], such as Egypt. JC will be maximised along with REF in the MOO. The mathematical formulations of the four objectives and their integration in the MOO are discussed further in this paper.

This paper adapts JC to the GC-HRES configuration under consideration by incorporating technology or energy source-specific job creation factors (JC factors) for each RES. JC is calculated by aggregating the creation of jobs across the manufacturing, installation, and operation & maintenance (O&M) phases of every RES in the GC-HRES. This paper critically examines the assumptions underlying these JC factors, discusses their advantages and limitations, and concludes with recommendations for their future refinement and application.

This paper will also provide a comprehensive and systematic analysis of how the inclusion of a social objective, along with technical, economic, and environmental objectives to the MOO reshapes the Pareto front and affects the optimal configuration of a GC-HRES. This detailed exploration of the compromises between the four objectives provides insights and conclusions that prior work has not extensively covered.

As stated previously, the study by [5] applied MOPSO to optimise the GC-HRES using technical, economic, and environmental objectives. This paper will extend the study by applying MOPSO after adding JC as a fourth social objective. The Non-Dominated Sorting Genetic Algorithm II (NSGA-II) will then be used to solve the expanded four-objective MOO problem. This paper will then perform a comparative analysis of both algorithms under the expanded set of objectives, examining the compromises among the objectives and how each algorithm shapes the Pareto front.

Although both algorithms are well-established, comparing their performance when a social objective is included offers valuable understanding into the how the different mechanisms that govern the performance of the algorithm affect its behaviour when the algorithm has to manage additional complexities. Such findings can guide future methodological developments.

This paper also includes a sensitivity analysis of the GC-HRES, through the investigation of how modifications to the battery constraints affect optimisation outcomes. This investigation will shed further light on the interplay between different objectives through these modifications, a topic rarely addressed in comparable literature. This investigation also enables an assessment of the impact of key parameters on algorithmic performance and overall GC-HRES design. The findings offer practical guidance and a nuanced understanding of the robustness and behaviour of the GC-HES design under varying conditions.

To the best of the authors' knowledge, no prior work has explicitly integrated Job Creation (JC) as an objective within the MOO of a GC-HRES. In existing GC-HRES studies, JC appears only as a post-optimisation metric, and where it is integrated as an objective in the MOO, it has been limited to standalone and off-grid HRES contexts. This study addresses this research gap and makes significant contributions to the field sustainable energy system optimisation with respect to the MOO of GC-HRESs using metaheuristic algorithms by:

- **First Job Creation (JC) integrated MOO framework for GC-HRES**: This study proposes the first MOO framework for a Grid Connected (GC)-HRES that explicitly integrates Job Creation (JC) as a social objective that is simultaneously optimised with LPSP, COE, and REF, thus elevating JC to the same level of importance as the other objectives. This paper presents a flexible MOO framework that can be readily replicated and adapted for other GC-HRES configurations, especially in terms of socially inclusive energy planning. This lays the groundwork for more sustainable and impactful GC-HRES designs.
- **Comprehensive Job Creation Factor quantification**: The adaptation and application of technology-specific JC factors across all phases of the renewable energy technology deployment process, enabling consistent and quantitative integration of the JC objective function into the MOO. The assumptions, advantages, limitations, and suggested improvements for future implementation are also documented.
- **Dual Metaheuristic Algorithm Analysis:** This study is one of the few studies to use NSGA-II (evolutionary) and MOPSO (swarm-based) metaheuristic algorithms to optimise a GC-HRES with JC as an explicit objective in the MOO. The study provides insights on the convergence behaviour, the solution diversity, and the computational efficiency under the added complexity of a fourth objective.
- **Impact of JC on the Pareto front**: This paper offers the first analysis of how the addition of JC reshapes the Pareto front and alters optimal GC-HRES component configurations, revealing new and unexplored compromises between social and techno-economic-environmental objectives. The analysis highlights how modest compromises in COE or LPSP can yield substantial gains in employment, making the results directly relevant for policy and investment decisions.
- **Constraint Sensitivity Analysis**: Through the variation of a key system constraint, the robustness of the GC-HRES design configuration and how constraint changes influence the balance among the four objectives is assessed. This provides information on the robustness and adaptability of the proposed GC-HRES configurations in different contexts.

The remainder of the paper is organised as follows: Section II is the *Background* which dives further into previous studies with the focus on JC integration and GC-HRES systems. Section III is *Mathematical Modeling* and focuses on the region of study and the mathematical modeling of the energy components and the objective functions. Section IV is the *Social objective function* and explores the formulation of quantification of JC as a social objective with the use of JC factors, Section V is the *Multi-objective optimisation* which details the MOO approach and includes the application of MOPSO, NSGA-II and TOPSIS and Section VI, the *Main findings and discussion of the MOPSO and NSGA-II optimisation* focuses on the main observations of the study and provides a detailed analysis of the results. The paper concludes with the *Conclusion*, *References*, and *Appendices A and B*.

II. BACKGROUND

A. THE EMERGING NEED TO INCLUDE SOCIAL OBJECTIVES

Including Job Creation (JC) as an explicit objective in the MOO of GC-HRESs is a novel approach motivated by the increasing emphasis on sustainable and fair energy transitions. Traditionally, developing the optimal HRES design configuration using MOO has focused on techno-economic and later environmental goals, such as minimising cost or emissions. A review study by Lian et al. on HRES sizing methodologies noted that 80% of HRES optimisation studies focused on reliability and economics. The study also urged that more attention should be paid to environmental and social objectives to realistically determine the impact of HRESs [7].

A study by Zhang et al. presented a more qualitative perception-based approach to the social impacts of HRESs. The social objective was modelled through social acceptance, a critical factor in ensuring the successful deployment of RESs. The study proposed a hybrid multi-attribute multi-objective decision making (MAMODM) framework for the optimisation of a renewable energy portfolio that directly incorporated public participation. The study highlighted that projects with RESs often face public resistance and addressed this by introducing a methodology to assess social acceptance, through multiple attributes such as affordability, noise, visual impact, and contribution to the region, which included employment opportunities (JC). JC was not treated as a primary optimisation objective. The study shows the importance of social considerations in RES system optimisation and the emergence of participatory models [8].

This sentiment was echoed in the study by Cuesta et al. where the authors emphasised the need for integration of social indicators in current HRESs modelling tools, which they argued was critical for designing resilient HRESs in small or remote communities. The lack of social indicators limited the ability of the tools to address broader sustainability goals. The study found that most existing modelling tools primarily considered technical, economic, and environmental parameters, while social dimensions, such as JC, social acceptance, community participation, and equity, were largely excluded from the optimisation processes. Only a couple of tools integrated qualitative or participatory elements [9]. Another review study by Farghali et al. identified JC as a key social benefit of RES deployment, along with other social outcomes, and noted that the quantification of social impacts, such as JC, remains underdeveloped compared to economic and environmental aspects. The review highlighted the need for better integration of metrics such as JC into optimisation models, such as MOO approaches, which can simultaneously address social, environmental, and economic domains [10].

Recently, however, there is growing recognition that criteria such as JC deserve direct consideration in the decision-making process, and therefore need to be explicitly considered in the optimisation process [11]. Integrating JC as an objective function in the MOO aligns energy planning with broader socio-economic goals, ensuring that HRESs contribute to local development and public well-being in addition to meeting energy and climate targets [11], [12]. This ideological shift reflects the broader energy policy context of a "just energy transition," wherein renewable energy deployment, through systems such as HRESs are leveraged to create jobs and foster community support for clean energy initiatives.

B. JOB CREATION (JC) AS A SOCIAL OBJECTIVE IN ENERGY SYSTEM OPTIMISATION AND PLANNING

The study by Sastresa et al. presented a methodological framework to assess the impact of renewable energy projects on the creation of local jobs, based on a case study in Spain. The study quantitatively estimated direct, indirect, and induced jobs created by the deployment of RESs, with a focus on wind energy, throughout the life cycle of RESs deployment, using JC factors and regional economic data to localise JC. The study argued that JC is a critical metric in the evaluation of projects that involve RESs [13]. Similarly, a study by Habibzadeh et al. presented a HRES sustainability assessment using a 4E framework: economic, environmental, exergy (technical) and social indicators for a system designed to power a petrochemical plant in Iran. The General Sustainability Indicator (GSI) integrated economic, environmental, and social indicators. The social indicators received the lowest weight in the Analytical Hierarchy Process (AHP) analysis, reflecting their lower prioritisation relative to environmental and economic dimensions. JC was not explicitly integrated as an optimisation objective, but indirectly contributed to the sustainability assessment via the GSI [14].

The study by Yalili et al. proposed a Multi-Objective Decision-Making (MODM) model to determine the optimal energy resource combination and capacity allocation for hybrid electricity generation systems, which have various combinations of renewable and non-renewable energy sources, in Türkiye. The optimisation model incorporated five conflicting objectives and involved the maximisation of JC, which was quantitatively formulated and integrated into the MODM alongside technical, economic, and environmental objectives. JC was integrated as a macro-level policy tool to inform government capacity allocation for different regions and was not related to the component sizing of the RESs in HRES configurations. The study provided a macro-level decision support model [15].

At a macro-level, increased renewable energy adoption has been empirically linked to higher employment. For example, an econometric analysis across the European Union (EU-28) from 2000 to 2016 found a statistically significant relationship between renewable power capacity and employment generation, estimating about 0.48% employment growth for each 1% increase in renewable capacity [12]. The employment effects were significant and supported the claims that renewable energy deployment encourages JC and economic development. The study is one of the few data-driven studies that empirically confirms the employment benefits of RESs deployment and thus adds quantitative evidence to policy claims that renewable energy supports labour markets.

The study by Ram et al. that modelled the employment impacts of transitioning to a 100% renewable global power system by 2050 reinforces this notion. The study found that RESs, especially solar PV, wind, batteries, and hydro-power, would replace fossil fuels while creating a significant number of jobs. The transition to 100% renewable electricity was projected to increase the total energy sector employment from 47 million (2015) to 62 million (2050). Solar PV and wind energy were found to be the largest contributors to the creation of jobs due to the high labour intensity required during the manufacturing, installation, and maintenance phases. The loss of jobs in fossil fuel sectors such as coal, oil, and gas due to RESs were more than offset by the jobs created by the renewable sector. The study also found that regions such as Africa, Asia, and Latin America benefited substantially from the jobs created by RESs, particularly if localised supply chains were developed. The study supported the notion that JC is a measurable, impactful, and significant outcome of RESs deployment [16].

C. MODELLING AND QUANTIFICATION OF JC IN HRES DESIGN OPTIMISATION

The typical methodological approach to model JC in HRES optimisation involves translating generated energy output or installed capacities of the renewable energy technologies under consideration into estimated employment. This is done by applying Job Creation (JC) factors with units such as jobs per MW or per MWh, which enables the optimisation algorithm to quantify the compromises between JC and other objectives [6].

One of the earliest examples of this approach is a study by Chauhan and Saini which modelled the potential of various RESs to create jobs in Chamoli, India. The study explored nine combinations of RESs to meet the energy demands of the village and considered economic and technical objectives with JC as the social objective. The study considered the potential for the creation of jobs at all stages of the project life cycle, including the construction, O&M and the decommissioning phases. The study provided a JC quantification method which included the potential of various renewable energy technologies to create jobs as fixed numerical values referred to as JC factors. The JC objective can be defined as the total number of jobs supported by the HRES, often measured in job-years over the lifespan of the HRES [6]. The method used to quantify JC and the JC factors were later cited in many other studies. The review study by Lian et al. stated that one of the most widely considered and crucial social objectives is JC, as the development of RESs often fosters growth in related industries, enhancing employment opportunities [7]. The study cites the method used by Chauhan and Saini to evaluate JC as an approach that can be generalised and used for various, if not all, possible HRES configurations [6], [7].

Similarly, a study by Hassan et al. on an off-grid HRES designed for a rural community in Bangladesh, considered three key objectives, namely COE, Lifecycle Carbon Emissions (LCE) and JC. Here, JC was also calculated across all phases of RESs deployment. The study integrated JC directly into the MOO and found that the optimal HRES configuration resulted in the estimated creation of 0.7396 jobs [17]. Furthermore, another study by Singh et al. proposed a MOO sizing model for an off-grid HRES that integrated six objectives and included the Human Development Index (HDI) and JC as social objectives. JC was calculated using JC factors and was explicitly optimised together with the other objectives. The optimal HRES configuration was found to create 0.2711 jobs [18]. Likewise, a study by Das et al. focused on a standalone HRES in Bangladesh that was to supply electricity to a community while also providing freshwater through a reverse osmosis (RO) desalination plant using the excess energy produced by the HRES. The MOO involved the maximisation of JC, which was quantified using JC factors for all RESs in the HRES and RO plant. The study found that employment could be increased by about 6% by explicitly favouring configurations that created jobs, with only modest cost compromises [19].

In addition, a study by Sawle et al. simultaneously addressed various technical and economic objectives, along with social objectives such as JC, HDI and particulate matter (PM) as a proxy for health impacts, which were integrated explicitly as quantitative objectives in the MOO for designing an off-grid HRES. The study was one of the first to explicitly include JC as an objective function in the MOO of an HRES and quantified JC using JC factors. The study reported that the JC factor of a particular renewable energy technology would improve over time as progress is made in the production of that renewable technology. This progress would result in a related increase in employment potential [20].

A study by Kushwaha et al. used the Employment Generation Factor (EGF), a metric similar to JC, related to employment potential and derived from component sizing and excess energy use. The study used the Socio-Techno-Economic-Environmental (STEE) approach which integrated EGF with other social factors, such as land cost and Human Progress Index (HPI), along with numerous technical, economic and environmental factors to design the optimal off-grid HRES to supply electricity to a rural village in India. However, the EGF was included as a post optimisation performance metric and not as a directly optimised objective [21]. In a similar and more recent study by Kushwaha et al., the focus was on the holistic optimisation of another off-grid HRES by incorporating the same set of STEE factors into the MOO for the HRES sizing. Again, the study treated EGF as one of several social indicators within a larger composite function and not as an explicit equal objective [22].

D. FOCUS ON GRID CONNECTED (GC)-HRES

A study by Shidhani et al. based in Indonesia focused on the integration of sustainability aspects in the planning of a regional power system expansion, which was abundant in fossil fuels and also had a large unexplored renewable energy potential. It was emphasised that the RES sector could create new jobs in a country with a large growing population, and thus, JC was included as the social objective, among the many economic and environmental objectives. The least expensive configuration used the smallest amount of land and was geared toward fossil fuel technologies. Configurations that emphasised minimal land use consistently favoured the use of fossil fuels. System configurations with RESs had lower carbon emissions and yielded higher renewable contributions and created more jobs. Despite numerous differences between various combinations of energy sources and technologies, each configuration still required the inclusion of fossil fuels to varying degrees to remain reasonably competitive [23]. This perhaps speaks to the need to include fossil fuels in HRES design, at least in the early stages of renewable energy system adoption, to ensure that these systems are reasonably competitive compared to their fully fossil fuel-powered counterparts. The most common way to include fossil fuels in HRESs is through the inclusion of a grid, such as a GC-HRES.

A two-stage framework for the sizing of a large GC-HRES in the Sokhna Industrial Zone of Egypt was developed by Elkadeem et al. The first stage involved the techno-enviro-socio-economic design optimisation of the GC-HRES, where JC was chosen as the social metric for a post-optimisation analysis, rather than an explicit objective in the optimisation loop. The study reported substantial social benefits that were quantified as the creation of nearly 10 new jobs [24]. Similarly, a study by Uyan focused on sizing a GC-HRES and used economic, environmental, and social performance metrics for the MOO. JC and external health cost reductions were the social metrics considered. Each GC-HRES configuration produced a different number of new jobs, which were quantified after the sizing of the configurations, as a post-optimisation impact metric rather than a driving objective in the optimisation process [25].

Similarly, a study by Abdoulaye et al. focused on a GC-HRES in the Massakory region and an off-grid HRES in the Mao region for the rural electrification through a techno-economic, environmental, and social assessment. The Massakory GC-HRES used economic and technical objectives, while the Mao HRES used an economic objective in the MOO. The post-optimisation analysis included social metrics such as JC and HDI that were calculated along with other technical and environmental metrics. Both the optimised off-grid and GC-HRES configurations created four new jobs [26].

Despite these emerging studies, incorporating JC into the MOO of HRESs is still an evolving area of research. An immediate challenge is the risk of compromise complexities between different objectives. For example, a configuration with more distributed solar power might create more local installation jobs but also significantly increase the energy cost. This would push the MOO to navigate the compromises between economic and social objectives. Techniques such as Pareto front analysis are appropriate for revealing these MOO compromises. Explicitly including JC in the MOO allows stakeholders to identify non-dominated solutions where a small increase in cost can yield a large gain in the creation of jobs, or vice versa. This empowers stakeholders to choose designs that align with sustainability and policy priorities. Recent reviews have highlighted that multi-criteria energy planning now increasingly considers social objectives such as JC alongside the traditional cost and reliability criteria [11].

Many of the reviewed studies demonstrated feasible ways to incorporate a quantitative, numerical JC metric into the optimisation model. This is a clear advancement over previous methods that did not include JC at all. However, some of the studies only evaluated JC after selecting an optimal HRES design through post-optimisation analyses. While the other studies integrated JC as an explicit optimisation objective in the MOO of off-grid and standalone HRES configurations. Interestingly, the review by Giedraityte et al. noted that while GC-HRESs were acknowledged and appeared in several studies, off-grid or standalone HRES were still the focus of most literature. GC-HRESs were considered an important research area, but often not coupled with deep social assessment [11].

E. NOVELTY OF THIS STUDY

The novelty of the research contained in this paper is the formulation of JC as a significant optimisation objective, elevating it to the same importance as an economic or technical objective, such as cost or reliability in the MOO and offering it the same leverage in the design process for the development of optimal GC-HRES configurations.

The design implications of explicitly including JC in the MOO of GC-HRES are significant. By quantifying JC within the MOO, stakeholders can directly evaluate the co-benefits of different energy technology combinations. For example, an optimal solution might not be the monetarily cheapest, but if it creates considerably more jobs and still meets emission targets, it could be the preferred solution for its socio-economic value. This approach supports more holistic sustainable development decisions, in which HRESs are evaluated not only in terms of energy generated and money produced, but also for their contribution to local livelihoods. It also improves community support and acceptance. The affected communities are more likely to support HRESs projects if they see clear employment gains, an insight reinforced by the positive link between local job creation and social acceptance of energy projects [11]. In strategic terms, making JC an explicit objective in the MOO helps to ensure that the deployment of GC-HRESs aligns with the global Sustainable Development Goals, such as affordable and clean energy, sustainable cities and communities, decent work and economic growth, and reduced inequalities and not just with climate goals. It formalises the notion of a fair, "just" energy transition by embedding workforce outcomes into the MOO and thus the design of energy systems.

In summary, the explicit inclusion of JC as an optimisation objective in the design of GC-HRESs is novel and valuable. It extends the conventional techno-economic paradigm to embrace a key social dimension of sustainability. Early research efforts, such as the earlier studies discussed in this paper, indicate that this integration is feasible and can yield insightful results. By highlighting and evaluating the compromises between technical efficiency, cost, environmental impact, and employment, a much richer basis for making decisions in energy planning can be developed. Ultimately, treating JC as an explicit objective moves GC-HRES optimisation toward a more comprehensive sustainability framework. A framework that balances technical efficiency with economic benefits with environmental sustainability and social prosperity. This approach contributes to energy systems that are not only technically and economically optimal but also socially inclusive and long-term beneficial.

III. MATHEMATICAL MODELING

A. AREA OF STUDY

As previously stated, the study by [5] explores the MOO of a GC-HRES in terms of technical, economic and environmental objectives using MOPSO. The system is located in Abu Atwa Village in Egypt. The area under consideration has ample renewable energy potential. It receives an average annual solar radiation of 1986 kWh/^{2} and an average wind speed of 3.7 m/s. The study used real on-site hourly electricity demand data, with an average demand of 463 kWh, a peak demand of 897 kW, and a load factor of 0.516 [5]. The GC-HRES under consideration integrates solar photovoltaic panels (PV), wind turbines (WT), battery storage banks (Bat), and the utility grid (G). The lifetime of the project is 25 years and the lifespan of the components is 25 years for solar panels and battery banks, and 15 years for wind turbines [5], [27].

B. MATHEMATICAL MODELING OF COMPONENTS

1) PHOTOVOLTAIC (PV) SYSTEM

The annual power output of the PV system (1) [28], [5]:

$$P_{PV} = \sum_{t=1}^{T} (P_{PVr} \times N_{pv} \times DF_{pv})(\frac{G(t)}{G_{base}}) \\ (1+K_T((T_{amb}(t)+G(t) \times (\frac{NOCT-20}{800} * 1000)-T_{base})) \quad (1)$$

where P_{PV} is the PV output power (kW), P_{PVr} is the rated module output (kW), N_{pv} is the number of PV modules, DF_{pv} is the PV derating factor (0.8), G is the global irradiance incident on the tilted plane (kW/m^2), and G_{base} is the solar radiation at reference conditions (1 kW/m^2). K_T is the temperature coefficient of the maximum power, where $K_T = -3.7 \times 10^{-3}$ (1/°C) for mono and poly-crystalline modules. T_{amb} is the ambient air temperature (°C), T_{base} is the temperature at reference conditions (°C), $NOCT$ is the normal operating cell temperature (°C), and T is the number of hours in a year (8760) [28]. This study considered the use of 30kW PV panels [5].

2) WIND TURBINE (WT) SYSTEM

The power generated by the WT system is largely dependent on the speed of the wind [5]. The annual WT system power output can be determined by (2) [29], [30] [5]:

$$P_{WT} = \left\{ N_{WT} \times \eta_W \times P_{WTr} \times \sum_{t=1}^{T} \left(\frac{V(t)^3 - V_{ci}^3}{V_r^3 - V_{ci}^3} \right), \\ V \leq V_r, \\ N_{WT}, \eta_W, P_{WTr}, V \leq V_r \leq V_c \\ 0, V_{co} \leq VorV \leq V_{ci} \right\} \quad (2)$$

where P_{WT} is the output power of the wind turbine (kW), N_{WT} is the number of wind turbines, η_W is the wind turbine efficiency, P_{WTr} is the rated power of the wind turbine (kW), T is 8760 hours, V_{ci} is the cut-in wind speed (m/s), V_{co} is the cut-out wind speed (m/s), V_r is the rated wind speed (m/s) and $V(t)$ is the upgraded wind speed (m/s) at the hub height $V(t)$ can be calculated using (3) [5]:

$$V(t) = V_r \left(\frac{H_{WT}}{H_r} \right)^{\alpha} \quad (3)$$

where H_{WT} is the wind turbine hub height (m), H_r is the reference height (m) and α is the friction coefficient, commonly at a value of (1/7) for low roughness surface and well-exposed sites [30]. This study considered the use of 50kW wind turbines in the GC-HRES [5].

3) BATTERY STORAGE BANK (BAT) SYSTEM

Once the load demand is met by the energy generated by the PV and WT systems, any surplus generated energy is stored in the battery storage bank (Bat) system. The Bat then supplies power to meet the load demand when the energy generated by the PV and WT systems is insufficient. The Bat considered in this study is a 1000 Ah, 48 kWh nickel iron battery [5].

The energy storage of the Bat is subject to the constraints detailed in equations (27), (28), (29) [5], [31] which are outlined in Appendix A. This study assumed a depth of discharge (DOD) of 80% and a that the usable energy of the Bat is 38.4 kWh, with the Bat discharging efficiency of 1 [5].

The Bat can only be charged by the energy generated on-site by the PV and WT systems of the GC-HRES [4]. The charging and discharging states of the Bat are calculated according to (4) and (5) respectively [5], [32].

$$C(t) = C(t-1) \times (1-\sigma) + P_{\text{sur}} \times \eta_b \quad (4)$$

$$C(t) = C(t-1) \times (1-\sigma) - P_{\text{def}} \quad (5)$$

where $C(t)$ is the battery charge at time t, $C(t-1)$ is the battery charge at the previous time step $t-1$ and σ is the self-discharge rate (energy the battery loses by itself without being used). This study assumed a 1% self-discharge per day, therefore σ per hour would be $0.01/24 \approx 0.0004167$ [5]. P_{sur} is the surplus power from the PV and WT systems that is available to charge the battery, P_{def} is the deficit power which is drawn from the battery to meet the load demand when there is not enough renewable power available from the PV and WT systems and η_b is the battery charging efficiency (amount of surplus energy that actually gets stored) set at 0.8 [5], [32].

4) GRID SYSTEM

When the PV and WT systems cannot supply the energy to meet the load demand and the Bat system cannot overcome this energy deficiency, the utility grid, modeled as an infinite energy source, will supply the energy necessary to meet the load demand [5]. The cost of the energy supplied by the grid is calculated using (6) [31]:

$$C_{grid} = C_p \times \sum_{t=1}^{8760} E_{grid\ purchased} \tag{6}$$

where C_{grid} is the cost of purchasing power from the utility (\$), $E_{grid\ purchased}$ is the purchasing power from the utility grid (kWh) and C_p is the cost of buying 1 kW from the grid at the local price (\$) [31], which in this study is 0.0425 \$/kWh for the region in which the GC-HRES is based [5]. The grid also absorbs any excess energy once the battery is fully charged [5]. This energy is sold to the grid and the income made from selling energy to the grid, can be calculated with (7) [31]:

$$R_{grid} = \sum_{t=1}^{8760} rate_{feed-in} \cdot E_{grid-selling} \tag{7}$$

where R_{grid} is the revenue from selling energy to the utility (\$), $E_{grid-selling}$ is the selling energy to the utility grid (kWh) and the $rate_{feed-in}$ is the feed-in tariff rate in the local area (\$) [31], which is considered to be 0.0617 \$/kWh in this study [5]. For further clarity, the architecture of the GC-HRES system is illustrated in Figure 1 [31].

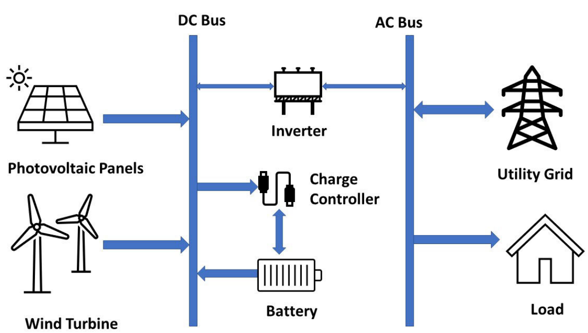

FIGURE 1. Grid-Connected Hybrid Renewable Energy System (GC-HRES) configuration adapted from [5], [31].

C. COMPONENT AVAILABILITY

The reliability of the GC-HRES to generate power is affected by the availability of the PV and WT systems, which can sometimes be affected by sudden failure or interruptions due to maintenance programs. The probability of availability (PA) is used to account for the unavailability of PV and WT systems. The PA is assumed to be 96% [5], [33], [34]. Therefore, the power generated by the PV and WT systems can be calculated by (8) [5], [33], [34].

$$P_{ren} = 0.96 \times (P_{PV} + P_{WT}) \tag{8}$$

where P_{ren} represents the available renewable power output considering the PA of 96%.

D. MATHEMATICAL MODELING OF THE OBJECTIVES

1) LOSS OF POWER SUPPLY PROBABILITY

The study considered technical, economic, and environmental objectives. The technical objective, Loss of Power Supply Probability (LPSP), evaluates system reliability by calculating the ratio of the total energy deficit to the total energy demand over a specified period [35]. Although GC-HRESs are generally more reliable than standalone systems, grid instability caused by blackouts or malfunctions can still affect the reliability of the power supply. Thus, assessing the LPSP for GC-HRESs is essential and is detailed in (9) [35]:

$$LPSP = \frac{\sum_{t=1}^{T} DE(t)}{\sum_{t=1}^{T} P_{load}(t)\Delta t} \tag{9}$$

where $LPSP$ is the loss of power supply probability, $DE(t)$ is the deficit energy at hour t, P_{load} is the load demand for period T [35]. T is 8760 hours and Δt is 1.

2) COST OF ENERGY (COE)

The economic objective, Cost of Energy (COE), measures the financial performance of the system and is derived from the lifetime of the project and the discounted cash flow analysis of each component (PV, WT, Bat) [5]. The Net Present Cost (NPC) of each component has to be evaluated before the COE can be calculated. The NPC of the PV system, NPC_{pv} , the NPC of the WT system NPC_{WT} and the NPC of the BAT system NPC_{BAT} [5] can be found in Appendix B. Once the NPC of the PV, WT and Bat systems have been calculated, the COE of the system can be evaluated according to (10) [36]:

$$COE = \frac{(CRF \times \sum_x NPC_x) + C_{grid} - R_{grid}}{E_{served} + E_{grid\ selling}} \tag{10}$$

where R_{grid} is the revenue from selling energy to the grid (\$), C_{grid} is the cost of purchasing power from the grid (\$), $E_{grid\ selling}$ is the selling energy to the grid (kWh), E_{served} is the primary load served ($kWh/year$), NPC_x is the net present cost of the PV, WT and Bat systems and CRF is the Capital Recovery Factor [36]. The CRF (\$) (used in (10)) evaluates the present value of a series of equal cash flows over the project lifetime and can be calculated using (11) [5]:

$$CRF = \frac{(\frac{I_r - I_f}{1+I_f})(1 + \frac{I_r - I_f}{1+I_f})^N}{(1 + \frac{I_r - I_f}{1+I_f})^N - 1} \tag{11}$$

where I_r is nominal interest rate of 15.25% and I_f is the inflation rate of 8.55% for the year 2019 for the region under consideration [5], [37].

3) RENEWABLE ENERGY FRACTION

The environmental objective, Renewable Energy Fraction (REF), quantifies the proportion of energy supplied by RESs to meet system demand in (12) [5]:

$$REF = \frac{\sum_{t=1}^{T}(P_{PV} + P_{WT}) \times \Delta t}{\sum_{t=1}^{T}(P_{PV} + P_{WT} + P_{grid\ purchased}) \times \Delta t} \quad (12)$$

where P_{PV}, P_{WT} is the power generated by the PV and WT systems, and $P_{grid\ purchased}$ is the power purchased from the grid.

4) GREENHOUSE GAS EMISSIONS

A lower REF indicates increased greenhouse gas (GHG) emissions as the grid relies on fossil fuels. This study also accounts for indirect life-cycle GHG emissions from the PV and WT systems. These emissions occur during the manufacturing, installation, and disposal phases of the PV and WT systems and should be accounted for despite the emission-free operation of the PV and WT systems. The GHG emissions from the grid and the PV and WT systems are calculated using (33), (34) and (35), respectively, with the total emissions of the GC-HRES determined by (36) [5]. To calculate the net savings of the GHG emissions caused by the GC-HRES, a base case calculation is required for comparison. The base case was assumed to be the scenario in which only the grid was used to meet the load demand of the village and can be found in (37). The net savings in GHG emissions can then be calculated by subtracting the total GHG emissions of the GC-HRES from the total emissions of the base case and is shown in (38) [5]. Refer to Appendix B for the complete mathematical formulation.

5) SYSTEM CONSTRAINTS

The system in this study operates under several constraints. The minimum and maximum bounds for the decision variables (components) in the GC-HRES are determined by the specific problem, including the number of variables and the complexity of the search space. This is represented by (39) [5] in Appendix B. Furthermore, the storage capacity and available energy of the battery are constrained, as outlined in (40) [31] in Appendix B. To ensure that the system is balanced, the total energy generated by all units must satisfy the system load demand over the entire scheduling period. For an hourly load demand and energy generation, the energy balance is shown in (41) [5] in Appendix B.

IV. SOCIAL OBJECTIVE FUNCTION

A. JOB CREATION

Evaluating the social impact of an energy system presents unique challenges, as it involves the quantification of abstract qualitative concepts. Job Creation (JC) within the context of HRESs, spans multiple stages, including component manufacturing, equipment transportation, installation, operation, and maintenance [7]. This study incorporates JC into the MOO of the proposed GC-HRES to highlight its social benefits and assess its influence on overall system performance.

B. JOB CREATION OBJECTIVE FUNCTION

The jobs created by the GC-HRES can be calculated using (13) [7], [6].

$$JC = JC_{PV}P_{PV} + JC_{wind}P_{wind} + JC_{Bat}E_{Bat} \quad (13)$$

where JC_{PV} is the number of jobs per MW of power generated by the PV system (jobs/MW), P_{PV} is the peak power generated by the PV system (MW), JC_{wind} is the number of jobs per MW of power generated by the WT system (jobs/MW) and P_{wind} is the maximum power generated by the WT (MW), JC_{Bat} is the number of jobs created per MWh of nominal capacity of the energy storage system (jobs/MWh); E_{Bat} is the nominal capacity of the energy storage system (MWh) [6]. This method of calculating JC was adapted from the equation by Chauhan and Saini [6] to evaluate the employment potential of the GC-HRES used in this study.

C. JOB CREATION FACTORS

Using the correct JC factors is an important aspect of calculating the employment potential of the GC-HRES. JC factors vary according to technology, job type, and project phase. The International Renewable Energy Agency (IRENA) defines direct jobs as employment directly related to core activities, such as manufacturing, construction, site development, installation, and O&M. These are measurable and scale proportionally to the growth of renewable technology. In contrast, indirect jobs involve secondary activities, such as raw material processing, marketing, administrative functions, and RESs research. Although direct jobs are universally included in JC studies, indirect jobs are less frequently quantified due to their complex dependencies on domestic manufacturing capacity and industry dynamics [38], [39].

The deployment of RESs comprises three key phases: manufacturing, installation, and O&M. Many studies combine manufacturing and installation into a single JC factor, obscuring individual impacts. However, distinguishing these phases is important, as installation jobs are often local, whereas manufacturing jobs may depend on an established domestic renewable technology industry. Studies that separate JC factors for these phases provide a more detailed understanding of their employment impacts. A higher overall JC factor is achieved when the individual JC values are combined to create a single aggregated JC factor of these two phases [39].

Notably, manufacturing and installation jobs are typically short-term and concentrated at the project's outset, measured in person-years per MW, where one person-year implies full-time employment for one person for a duration of a single year. This reflects the transient nature of these jobs. However, O&M jobs are long-term and span the project lifetime, measured in jobs per MW. The difference in units expertly reflects the varied nature of the jobs in each phase. However, the difference in units also complicates the comparison of the job creation capacity between phases. To evaluate the total JC potential, the JC factors across all phases must be aggregated into a common unit of measurement [39].

A standardised approach by Kammen et al. [40] and Wei et al. [41] averaged the manufacturing and installation jobs over the project lifetime by converting them into O&M equivalent units (jobs/MW). The continuous growth of renewable energy plants in any economy justified this approach. Ultimately, suggesting that a JC factor, averaged over a project lifetime, is a fair representative measure of the ongoing labour in the manufacturing and installation HRES stages [39], [40].

This study only considered direct jobs, given the limited available data on indirect job creation of RESs [38], [39]. The JC factors used are shown in Table 1 [39], with maximum values applied to reflect the highest employment potential for each RES in the GC-HRES. The minimum and median values were excluded to align with the assumption of maximum job creation in the given scenario [39].

TABLE 1. Job Creation Factors for PV and Wind at different phases of energy technology deployment.

RES	Manufacturing person-years/MW	Installation person-years/MW	O&M jobs/MW
PV	34.5	33	1.65
WT	12.5	6.7	0.7
RES	Manufacturing jobs/MW	Installation jobs/MW	O&M jobs/MW
$PV_{normalised}$	1.38	1.32	1.65
$WT_{normalised}$	0.5	0.27	0.7

Table 1 outlines the JC factors for PV and WT systems for each phase. JC factors are provided in raw and normalised units in Table 1. The raw JC factors for PV: 34.5 person-years/MW and 33.0 person-years/MW for the manufacturing and installation phases, as well as 1.65 jobs/MW for the O&M phase were found in a review by Cameron et al. The raw JC factors for WT: 12.5 person-years/MW and 6.7 person-years/MW for the manufacturing and installation phases, as well as 0.7 jobs/MW for the O&M phase were also found in a review by Cameron et al. [39].

Normalised values were adjusted the for the 25-year GC-HRES project lifetime using the approach of Kammen et al. [40] and Wei et al. [41], where the values for the manufacturing and installation phases were averaged over the project lifetime, thus converting them into O&M equivalent units (jobs/MW). The normalised values for the manufacturing, installation and O&M phases for the PV and WT systems can be found in the last two rows of Table 1. Normalised values were found by dividing the raw values by the project lifetime (25 years).

The tabulated data shows that the PV system has significantly higher JC factors than the WT system across all phases. In PV systems, the manufacturing and installation phases create a similar number of jobs, whereas WT systems see nearly double the jobs in manufacturing compared to installation. When normalised, the O&M phase of both RESs shows greater employment potential than the individual manufacturing or installation phases.

For the PV system, combining the manufacturing and installation phases results in a JC factor higher than O&M, while for the WT system, the combined value aligns closely with the O&M phase. This suggests greater consistency in job creation across WT phases compared to the PV phases, where job potential is concentrated in the installation and manufacturing phases.

Aggregating normalised JC factors yields a final value of 4.35 jobs/MW for the PV system and 1.47 jobs/MW for the WT system. Thus, the energy generation of the PV system creates nearly three times more jobs than the WT system per MW of installed capacity. The final JC factors used in (13) are 4.35 jobs/MW for JC_{PV}, 1.47 jobs/MW for JC_{wind} [39], and 0.01 jobs/MWh for JC_{Bat} [20]. These values align with the findings of [20] and [39], which emphasise the dominance of O&M in job creation for the WT system compared to the PV system.

V. MULTI-OBJECTIVE OPTIMISATION

This study aims to determine the optimal number of components, N_{PV}, N_{WT} and N_{Bat} to satisfy the technical, economic, environmental, and social objectives of the GC-HRES. Metaheuristic algorithms are used to minimise the COE and LPSP objectives while maximising the REF and JC objectives [5], to obtain a set of non-dominated solutions. The objectives of the GC-HRES can be expressed as a vector-valued function:

$$f(X_i) = [minLPSP(X_i), minCOE(X_i), maxREF(X_i), maxJC(X_i)] \tag{14}$$

This function was formulated as a minimisation based function and thus the objectives that need to be maximised were negated to fit into a unified minimisation function:

$$f(X_i) = [LPSP(X_i), COE(X_i), -REF(X_i), -JC(X_i)] \tag{15}$$

As there are four objectives, each objective must have a weight to illustrate the relative importance of each objective in the MOO. Thus, the multi-objective formulation can be expressed as a scalar aggregation using a weighted sum.

$$\begin{aligned} Fitness(X_i) = {} & w_{LPSP} \times LPSP(X_i) + w_{COE} \times COE(X_i) \\ & + w_{REF} \times (-REF(X_i)) + w_{JC} \times (-JC(X_i)) \end{aligned} \tag{16}$$

All four objectives are weighed equally in the MOO. Equal weights for each objective were chosen so as to reflect the balanced importance of technical, economic, environmental, and social objectives, ensuring no single objective dominated the optimisation:

$$w_{LPSP} = w_{COE} = w_{REF} = w_{JC} = w = 0.25 \tag{17}$$

The function can be simplified to:

$$\begin{aligned} &Fitness(X_i) \\ &= w \cdot (LPSP(X_i) + COE(X_i) - REF(X_i) - JC(X_i)) \end{aligned} \tag{18}$$

Subject to the following decision variable bounds [5]:

$$N_x^{\min} \leq N_x \leq N_x^{\max}, x \in \{PV, WT, BAT\} \tag{19}$$

MOO problems involve optimising multiple conflicting objectives subject to constraints. A generic MOO formulation is given below [23]. Minimise or maximise:

$$f_m(x), m = 1, 2, \ldots, M$$

Subject to:

$$\begin{aligned} g_j(x) &\geq 0, j = 1, 2, \ldots, J \\ h_k(x) &= 0, k = 1, 2, \ldots, K \\ x_i^L &\leq x_i \leq x_i^(U)l = 1, 2, \ldots, n, \end{aligned}$$

where $x \epsilon R^n$ represents a vector of n decision variables $x = (X_1, X_2, \ldots, X_n)^T$, and the feasible decision space $S \subset R^n$ includes all solutions that meet the constraints [23]. The objective space $Z \subset R^M$ is comprised of the objective functions and maps every x in S to a corresponding point $z \epsilon R^M$. The process of sorting these solutions identifies non-dominated solutions, also known as Pareto-optimal solutions (POS), where no objective can be improved without worsening at least one other [42].

A. MULTI-OBJECTIVE PARTICLE SWARM OPTIMISATION (MOPSO) ALGORITHM

The MOO was solved using the Multi-Objective Particle Swarm Optimisation (MOPSO) algorithm, adapted from the procedure implemented in [5], for minimising LPSP and COE and maximising REF. As this procedure is comprehensively detailed in [5], this paper focuses on the modifications introduced and a performance comparison between the MOPSO and NSGA-II algorithms.

The PSO mechanism, inspired by natural swarm behaviour, was introduced by Kennedy and Eberhart in 1995. In MOPSO, particles exchange information and move toward the global best solutions. An external repository is employed to store the non-dominated population solutions, which are updated iteratively. At the local level, dominance rules and probabilistic mechanisms determine the personal best particles, guiding the evolution of the swarm [43].

The MOPSO implementation steps are outlined in Algorithm 1, which details the initialisation, selection, crossover, and mutation processes and is adapted from [5]. The terms in Algorithm 1 stand for: N_{Pop} is the population size, N_{Rep} is the repository size, w and w_{damp} are the inertia weight and inertia weight damping ratio respectively, c_1 and c_2 are the personal and global learning coefficients respectively, r_1 and r_2 are random numbers sampled independently of a uniform distribution in the range 0 to 1, β is the leader selection pressure, λ is the deletion selection pressure, μ is the mutation rate, and $Max_{iteration}$ is the maximum number of iterations.

B. NON-DOMINATED SORTING GENETIC ALGORITHM ii (nsga-ii)

The Non-Dominated Sorting Genetic Algorithm II (NSGA-II) was chosen for the MOO of the GC-HRES in this study due to its high optimisation speed, robust search capabilities, and proven reliability in benchmark MOO problems [44]. Its elite strategy ensures precision and accuracy in the optimisation process. The crowding distance operator maintains solution population diversity during optimisation, which is crucial for a MOO addressing conflicting objectives [42].

Introduced in 2002 in the seminal work, *A Fast and Elitist Multi-Objective Genetic Algorithm: NSGA-II* [45], the algorithm employs tournament selection, crossover, and mutation to generate child solutions from an initial population of parent solutions. The parent and child solutions undergo non-dominated sorting and crowding distance sorting, selecting the best solutions for the next generation. These are the two defining steps of the elitist genetic algorithm approach, promoting rapid convergence to the Pareto-optimal front [44].

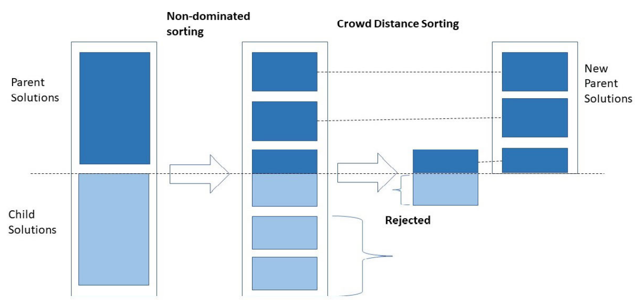

FIGURE 2. NSGA-II Process based on an illustration by [44].

NSGA-II balances exploration and exploitation by favouring high-fitness solutions while maintaining population diversity through controlled selection. The algorithm's dual focus on fitness and diversity ensures efficient convergence to a diverse and well-distributed set of non-dominated solutions [23]. The NSGA-II process is illustrated in Figure 2 [44]. In this study, the NSGA-II algorithm was implemented using the *pymoo: Multi-objective optimisation in Python* framework. *pymoo* is a versatile Python library for single and multi-objective optimisation [46]. The framework was customised to suit the GC-HRES model, with the chosen specifications outlined in Table 2 [46]. Notably, pymoo inherently handles minimisation problems. Therefore, to address the requirement of maximising REF and JC, these objectives were negated, transforming the problem into minimising

Algorithm 1 Implementation of MOPSO

1:Set MOPSO parameters: $N_{Pop} = 200$, $N_{Rep} = 200$, $w = 0.5$, $w_{damp} = 0.99$, $c_1 = 1.8$, $c_2 = 2$, $\beta = 2$, $\lambda = 2$, $\mu = 0.1$, $Max_{iteration} = 100$

2:Set variable boundaries for N_{PV}, N_{WT}, and N_{Bat} $N_{PV} \in [0, 50]$, $N_{WT} \in [0, 50]$, $N_{Bat} \in [0, 100]$

3:Initialise repository $Rep = \varnothing$

4:for each particle $i = 1$: N_{Pop} do

5: Randomly initialise particle population with positions X_i and velocities V_i

$$X_i = [N_{PV}, N_{WT}, N_{Bat}] = 0$$
$$V_i = 0$$

6: Evaluate fitness as:

$$\text{Fitness}(X_i) = w_{LPSP} \times \text{LPSP}(X_i) + w_{COE} \times \text{COE}(X_i) - w_{REF} \times \text{REF}(X_i) - w_{JC} \times \text{JC}(X_i)$$

Find index of the best particle

$$P_{best,i} = X_i$$

7: endfor

8: Update repository Rep with non-dominated solutions

$$Rep = Dominance(P_{best})$$

9: k = 0 (start iteration counter)

10: While$k \le Max_{iteration}$

11: for $i = 1$: $NPop$

12: Select Leader from Rep

$$leader = selectleader(Rep)$$

13: Update particle velocity and position

$$V_i^{k+1} = \omega V_i^k + c_1 r_1 (P_{best,i}^k - X_i^k) + c_2 r_2 (\text{Leader}_i^k - X_i^k)$$
$$X_i^{k+1} = X_i^k + V_i^{k+1}$$

14: Evaluate fitness using fitness function

15: Apply mutation

$$X_i = Mutate(X_i)$$

16: ifX_i dominates $P_{best,i}$then Update $P_{best,i} = X_i$

17: endif

18: endfor

19: Update repository Rep with non-dominated solutions

20: Update inertia weight w

$$w = w \times w_{damp}$$

21: if $k < Max_{iteration}$ then

22: $k = k + 1$ and go to Step 10

23: else

24: Go to Step 14

25: end if

26: end while

negative REF and negative JC, indirectly maximising these objective functions [46].

TABLE 2. NSGA-II specifications for pymoo.

Criteria	Specification	Purpose
Algorithm	NSGA2	NSGA-II is *NSGA2* in *pymoo*
Population Size	200	Aligns with MOPSO setup for fair comparison
Number of Offspring	200	Matches population size for full generational replacement
Sampling	Random Sampling	Wide initial exploration
Crossover	SBX (prob=0.9, η=15)	Frequent recombination, maintains parent characteristics
Mutation	PM(η =20)	Adds variability without extreme deviations
Termination	100	Aligns with MOPSO setup for fair comparison

The NSGA-II algorithm is referred to as *NSGA2 pymoo* [46]. The population size of 200 and the termination criteria of 100 iterations were chosen to match the MOPSO conditions [5]. The number of offspring was chosen as 200 to match the population size for a full generational replacement [46] and to balance sufficient exploration and exploitation of the solution space. Random Sampling promotes uniform distribution across the search space by providing diverse starting points without prior knowledge of the landscape, enabling initial wide exploration and preventing premature convergence [46] [48].

The *Simulated Binary Crossover* (SBX) was used with a probability of 0.9 and a distribution index (η) of 15. The high crossover probability encourages frequent recombination, enhancing exploration while preserving some parent solutions. The η value of 15 strikes a balance between exploration (low η) and exploitation (high η), generating offspring moderately spread from their parents, and hence is effective for diverse MOO systems [46], [48].

The *Polynomial Mutation* (PM) with a distribution index (η) of 20 was applied. PM follows the same probability distribution as the SBX. This choice supports the fine-tuned exploration of the search space, especially for continuous decision variables such as PV, WT, and Bat. The final values of the decision variables were rounded up to the nearest discrete value. A moderate η of 20 ensures controlled perturbations, promoting variability while maintaining convergence to the Pareto front, thereby ensuring that *NSGA2* explores the search space without significantly deviating from promising regions [46], [48].

The NSGA-II implementation steps are outlined in Algorithm II, which details the initialisation, selection, crossover, and mutation processes. The terms in Algorithm II stand for N_{pop} is the population size, $N_{\text{offspring}}$ is the number of offspring, $N_{\text{termination}}$ is the termination criteria, which is the maximum number of generations (iterations), g is generation, X_i^g is the selected parent solution, the i^{th} parent at g,P^g is the current population at g, X_{p1} and X_{p2} are the two parent

Algorithm 2 Implementation of NSGA-II using pymoo

1: Set NSGA-II parameters: $N_{\text{pop}} = 200$, $N_{\text{offspring}} = 200$, Crossover: SBX($p = 0.9$, $\eta = 15$), Mutation: PM($\eta = 20$), $N_{\text{termination}} = 100$
2: Set variable boundaries for N_{PV}, N_{WT}, and N_{Bat}: $N_{PV} \in [0, 50]$, $N_{WT} \in [0, 50]$, $N_{Bat} \in [0, 100]$
3: Generate initial population of N_{pop} using Random Sampling
4: Evaluate fitness as:
$$\text{Fitness}(X_i) = w_{LPSP} \times \text{LPSP}(X_i) + w_{COE} \times \text{COE}(X_i) - w_{REF} \times \text{REF}(X_i) - w_{JC} \times \text{JC}(X_i)$$
5: Apply initial non-dominated sorting to rank each solution X_i based on Pareto dominance:
$$\text{Rank}(X_i) \text{ based on Pareto dominance}$$
6: Calculate the initial crowding distance for each solution X_i to assist parent selection for the first generation:
$$d_i = \sum_{m=1}^{M} \frac{f_m(X_{i+1}) - f_m(X_{i-1})}{f_m^{\max} - f_m^{\min}}$$
{Distance is used to select less crowded solutions to ensure diversity}.
7: **for** each generation $g = 1{:}\ N_{\text{termination}}$ **do**
8: Select parent solutions using pymoo's default binary tournament selection [45]:
$$X_i^g = \text{TournamentSelect}(P^g)$$
9: Apply SBX crossover to generate offspring solutions: {Conceptually, offspring can be represented as}:
$$X_{\text{child}} \approx 0.5 \times ((1+\beta) \times X_{p1} + (1-\beta) \times X_{p2}$$
{However, SBX generates offspring using a probabilistic distribution defined in [49]}.
10: Apply Polynomial Mutation to offspring solutions: {Mutation perturbs solution by adding a small change ΔX, based on a polynomial probability distribution [45]}
$$X_{\text{mutated}} = X + \Delta X$$
11: Evaluate fitness of offspring solutions using the fitness function
12: Combine parent and offspring solution populations
13: Apply non-dominated sorting to rank combined parent and offspring solutions into Pareto fronts, as in Step 5.
14: Recalculate crowding distance for each solution X_i in the Pareto front as in Step 6.
15: Select the best N_{pop} solutions for the next generation based on rank and crowding distance
16: **end for**
17: Post-process final N_{pop} by rounding decision variables to the nearest integer values
18: Return the final non-dominated set of solutions representing the Pareto-optimal front

solutions selected for crossover, β is the crossover coefficient derived from a probability distribution controlled by the distribution index (η), X_{child} is the new offspring generated as a combination of the two parent solutions, X is the current solution before mutation, ΔX is the perturbation added to the solution, $X_{mutated}$ is the new solution after mutation, d_i is the crowding distance of solution X_i, m is the objective index, ranging from 1 to M where M is the number of total objectives, f_m is the objective function for the m^{th} objective, X_{i+1} and X_{i-1} are the neighbouring solutions of X_i in the sorted list of solutions, $f_m(X_{i+1})$ and $f_m(X_{i-1})$ are the objective function values of the neighbouring solutions for objective m and f_m^{max} and f_m^{min} are the maximum and minimum values of objective m among all solutions in the same Pareto front.

The use of NSGA-II and MOPSO as the two main algorithms for the MOO of the GC-HRES is deliberate and justified. MOPSO is inspired by swarm intelligence and operates through the collective behaviour of particles using velocity and position updates based on leader particles and personal best solutions, offering faster convergence and simplicity in tuning parameters [50]. Conversely, NSGA-II, an evolutionary algorithm, uses genetic operators such as selection, crossover, and mutation along with non-dominated sorting and crowding distance to maintain population diversity while converging toward the Pareto front. It has become a benchmark in MOO problems for its ability to effectively approximate diverse balanced compromise solutions in highly non-linear problem spaces [45]. The complementary nature of these two algorithms, swarm-based versus evolutionary, adds methodological rigour by capturing different search dynamics and helping validate the generality of the obtained Pareto-optimal solutions.

Importantly, both algorithms are population-based and do not require gradient information, enabling them to handle the non-convexity, discontinuities, and mixed integer variables that are characteristic of GC-HRES design problems [18], [51]. Unlike deterministic methods such as linear programming or goal programming, which often assume smooth and convex landscapes, NSGA-II and MOPSO can effectively navigate complex MOO spaces without simplifying assumptions [52]. Their effectiveness has been demonstrated in energy systems that integrate RESs, such as the application of NSGA-II to optimise RES-integrated microgrids and off-grid systems [17], while PSO and its variants are noted for their speed and efficiency in solving large-scale sizing and energy dispatch problems [18], [19]. Using both algorithms, this study not only gains comparative insights into convergence speed, solution diversity, and computational efficiency, but also ensures that its findings are not dependent on the algorithm, thereby enhancing their credibility and the ability to generalise the domain of GC-HRES design optimisation.

C. TECHNIQUE OF ORDER OF PREFERENCE BY SIMILARITY TO IDEAL SOLUTION (TOPSIS)

Once the Pareto-optimal (non-dominated) solutions of the MOPSO and NSGA-II algorithms were obtained, the best solution from the Pareto front had to be identified.

The Technique of Order of Preference by Similarity to Ideal Solution (TOPSIS), a Multi-Criteria Decision Making (MCDM) method developed by Hwang and Yoon in 1981 was employed to achieve this [53]. TOPSIS is widely used in MOO problems due to its simplicity, ability to handle objectives of varying magnitudes, and minimal input requirements [44].

TOPSIS ranks solutions based on their relative distance to two hypothetical solutions. The Positive Ideal Solution (PIS) represents the best possible values for each objective, such as the maximum values for the REF and JC objectives and the minimum values for the LPSP and COE objectives. The Negative Ideal Solution (NIS) represents the worst possible values for each objective. A solution is considered optimal if it is closest to the PIS and farther away from the NIS [44]. The algorithm to implement TOPSIS is detailed in the following five steps [54]:

Step 1 Normalised objective matrix is constructed with m rows (Pareto-optimal solutions) and n columns (objectives) by applying the relationship in (20) [54]:

$$F_{ij} = \frac{f_{ij}}{\sqrt{\sum_{i=1}^{m} f_{ij}^2}} \tag{20}$$

where f_{ij} is the ith value of the jth objective in the objective matrix and F_{ij} is the value of f_{ij} after normalisation [54].

Step 2 Multiply each column by its corresponding weight to account for the relative importance of objectives to construct a weighted normalised objective matrix as shown in (21) [54]:

$$v_{ij} = F_{ij} \times w_j \tag{21}$$

where v_{ij} is the weighted value or rank of F_{ij} and w_j is the weight of the jth objective [54].

Step 3 Determine the PIS (A^+) and NIS (A^-). The best value for each objective is found mathematically with (22) [54]:

$$\begin{aligned} A^+ &= \{(Max_i(v_{ij})l_j \in J), \\ &\quad Mini(v_{ij})l_j \in J')li \in 1, 2, \ldots, m\} \\ &= \{v_1^+, v_2^+, v_3^+, \ldots, v_j^+, \ldots, v_n^+\} \end{aligned} \tag{22}$$

where J is the set of maximisation objectives, J' is the set of minimisation objectives from the total set of 1, 2, 3, 4, …, n. In practical terms, this is the largest value within the column of the objective matrix for the maximisation objective and the smallest value in the column for the minimisation objective [54]. The negative ideal solution is found in the opposite way and can be mathematically given by [54] (23):

$$\begin{aligned} A^- &= \{(Min_i(v_{ij})l_j \in J), \\ &\quad Maxi(v_{ij})l_j \in J')li \in 1, 2, \ldots, m\} \\ &= \{v_1^-, v_2^-, v_3^-, \ldots, v_j^-, \ldots, v_n^-\} \end{aligned} \tag{23}$$

Step 4 The Euclidean distance of each solution from the PIS (S_{i+}) and the NIS (S_{i-}) is calculated in (24) and (25) [54]:

$$S_{i+} = \sqrt{\sum_{j=1}^{n} (v_{ij} - v_j^+)^2}\ i = 1, 2, 3, \ldots, m \tag{24}$$

$$S_{i-} = \sqrt{\sum_{j=1}^{n} (v_{ij} - v_j^-)^2}\ i = 1, 2, 3, \ldots, m \tag{25}$$

Step 5 The closeness of each optimal solution is calculated by [54]:

$$C_i = \frac{S_{i-}}{S_{i-} + S_{i+}} \tag{26}$$

The solution with the largest C_i is closest to the PIS and is the optimal choice [54]. By following these steps, TOPSIS ranks the Pareto-optimal solutions based on their proximity to the ideal point, providing a structured approach for selecting the most balanced solution.

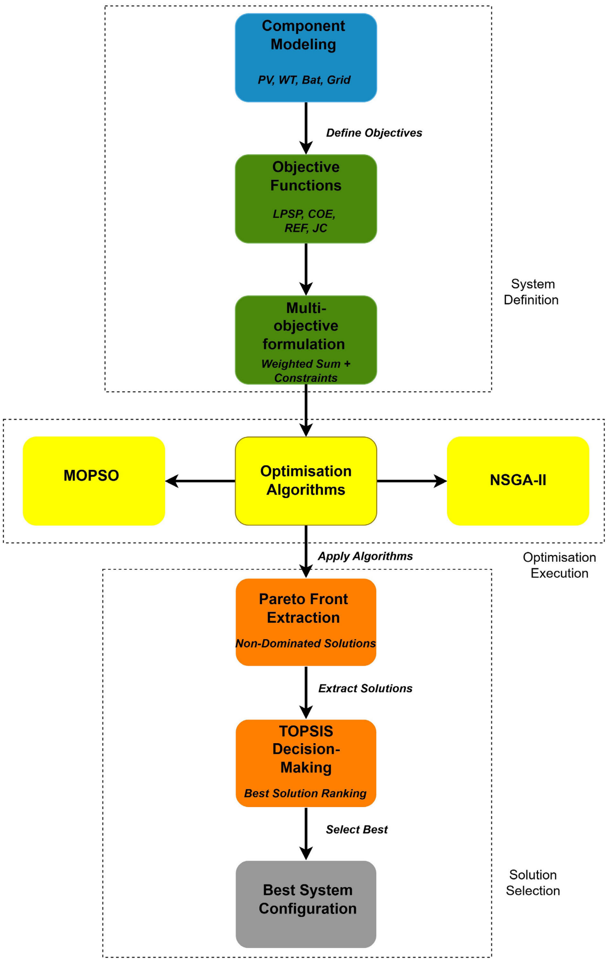

FIGURE 3. Integrated methodological framework for the MOO of the GC-HRES.

D. INTEGRATED METHODOLOGICAL FRAMEWORK

The Figure 3 illustrates the integrated methodological framework applied in this study for the MOO of the GC-HRES. The framework is structured into three main phases: *System Definition, Optimisation Execution, and Solution Selection*.

The *System Definition* phase involves the modelling of the components of the GC-HRES, the PV, WT, Bat and Grid as well as the four objective functions, the LPSP, COE, REF, and JC. These objectives are formulated into an equal weighted MOO problem, incorporating system constraints.

The *Optimisation Execution* phase applies MOPSO and NSGA-II to explore the solution space and generate non-dominated Pareto-optimal solutions. In the *Solution Selection* phase, the extracted Pareto front is analysed using TOPSIS. This process identifies the best system configuration, the best non-dominated optimal number of PVs, WTs, and Bats, that balances technical, economic, environmental, and social objectives.

This framework provides a systematic approach to optimise complex GC-HRES, supporting stakeholders in selecting balanced and sustainable solutions.

VI. MAIN FINDINGS AND DISCUSSION OF THE MOPSO AND NSGA-II OPTIMISATION

A. IMPACT OF INCLUDING JOB CREATION (JC) AS A FOURTH OBJECTIVE

Multiple tests were performed to evaluate and compare the performance of the MOPSO and NSGA-II algorithms for the MOO of the GC-HRES. Initially, the MOO was replicated following the methodology outlined in [5] which optimised LPSP, COE, and REF. These results (*Replicated MOPSO*) were compared to those of the original study (*Original Study*) by [5].

After successfully replicating the study, JC was introduced as an additional objective (*MOPSO with JC*) to evaluate its impact on the results. The same optimisation tasks were performed using NSGA-II. A MOO without JC (*NSGA-II*) and another MOO with the inclusion of JC (*NSGA-II with JC*). The average LPSP, REF, COE and JC values are summarised in Table 3.

TABLE 3. The Average LPSP, REF, COE and JC values for each test cases.

Average	Original Study	Replicated MOPSO	MOPSO with JC	NSGA-II	NSGA-II with JC
LPSP	0,004	0,015	0,027	0,000	0,010
REF(kW)	0,461	0,548	0,556	0,400	0,398
COE($/kWh)	0,042	0,050	0,051	0,036	0,034
JC(Jobs)	0,000	0,000	6,801	0,000	4,904

To create a visual comparison across all test cases, the results in Table 3 were illustrated using a heatmap in Figure 4 and a radar chart in Figure 5. To allow a meaningful comparison between objectives that have different units and magnitudes, the values of LPSP, REF, COE, and JC in Table 3 were normalised. This approach ensured that each objective contributed equally to the heatmap, regardless of its original scale. The normalised values of the minimisation objectives, LPSP and COE, were adjusted using the complement transformation, thus ensuring that higher heatmap values consistently represented better performance across all objectives. The heatmap in Figure 4 visually highlights how each test case performed relative to others for each objective.

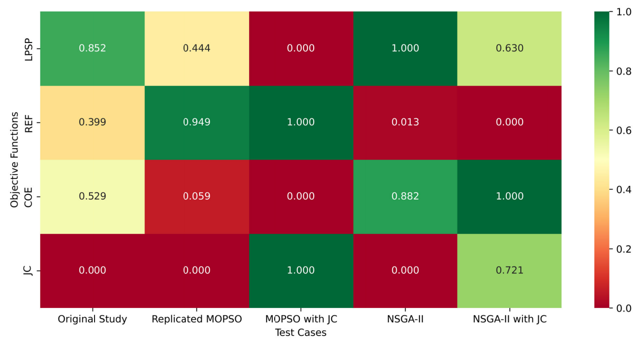

FIGURE 4. Heatmap illustrating the normalised LPSP, REF, COE, and JC objectives across different test cases.

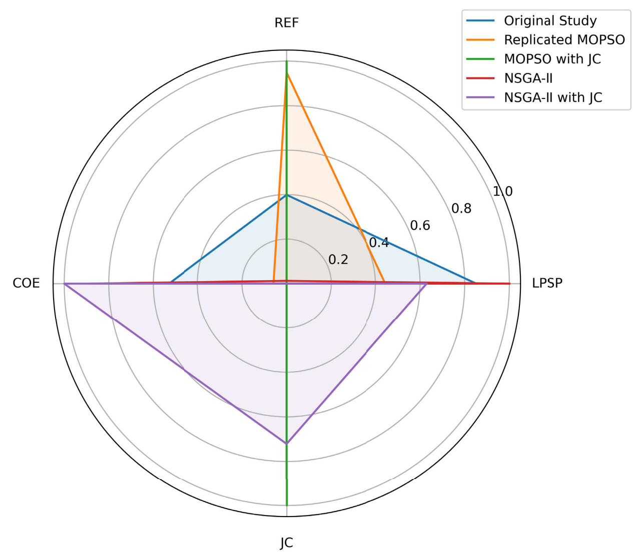

FIGURE 5. Radar chart showing the normalised performance of LPSP, REF, COE, and JC for each test case.

The Pareto (non-dominated) optimal solution for the objective functions, along with the optimal component configurations, NPC, and GHG are given in Table 4.

The values in Table 4 were visually summarised using a heatmap, Figure 6 and a stacked bar chart, Figure 7 to enhance the interpretation of the results. The heatmap in Figure 6 illustrates the normalised Pareto-optimal values of the variables LPSP, REF, COE, JC, GHG, and NPC for each test case. Similarly as in Figure 4, the normalised values for the minimisation objectives and the variables NPC and GHG (variables that favour lower values during optimisation) were inverted, thus ensuring that higher values

TABLE 4. Pareto Optimal Solutions and Component Configurations.

Variable	Original Study	Replicated MOPSO	MOPSO with JC	NSGA-II	NSGA-II with JC	Battery Constraint MOPSO
LPSP	0,000	0,000	0,031	0,003	0,014	0,017
REF(kW)	0,401	0,400	0,405	0,409	0,405	0,441
COE($/kWh)	0,032	0,031	0,051	0,046	0,041	0,061
JC(Jobs)	0,000	0,000	4,234	0,000	4,492	0,000
GHG(ton)	549697	565211	546685	538602	548649	515401
NPC($)	1808583	1853748	2864127	2689427	2343234	3457075
nPV	40	41	40	30	36	28
nWT	0	0	1	23	10	35
nBat	0	0	19	1	3	5

on the heatmap are indicative of better performance across all variables. Figure 7 compares the Pareto-optimal component configurations, namely the number of PVs, WTs and Bats, across all test cases. The chart reveals clear shifts in system design priorities depending on the optimisation setup. The stacked bar graph highlights how varying objectives and constraints influence the GC-HRES architecture.

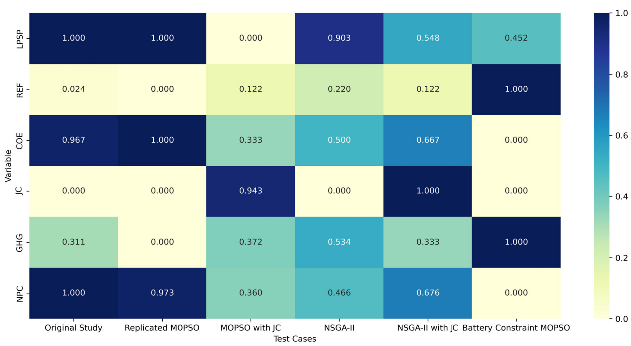

FIGURE 6. Heatmap presenting the normalised Pareto-optimal values of LPSP, REF, COE, JC, GHG, and NPC across text cases.

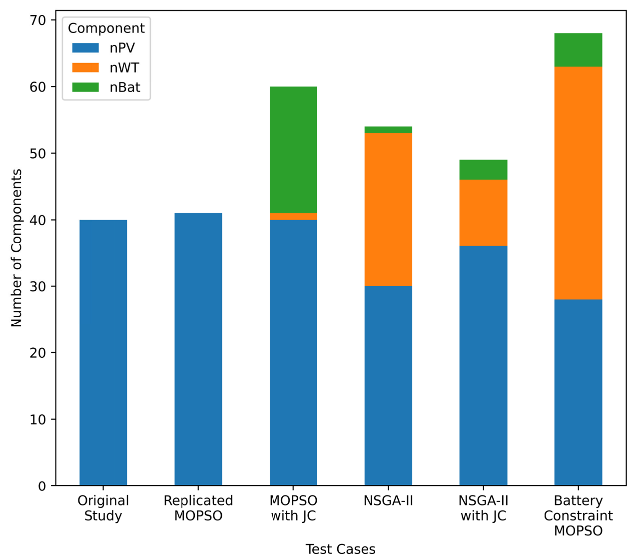

FIGURE 7. Stacked bar chart comparing the number of PV panels, wind turbines, and battery bank components in the optimal configurations for each test case.

Including JC as a fourth objective in the MOO framework changes the solution space dynamics, as evident from Table 3 and Table 4. In Table 3, MOPSO achieved a higher average JC (6,801) than NSGA-II (4,904), suggesting its tendency to favour configurations with increased RESs to increase employment potential. The average REF corresponding values of MOPSO (0,556) and NSGA-II (0,398) support this. This trend is observed for the algorithms in both cases (*without JC* and *with JC*). However, the difference in the average REF values is greater when JC is included.

REF values in Table 4 remained consistent with a slight increase in MOPSO (0,400 to 0,405) and a decrease in NSGA-II (0,409 to 0,405) after including JC, suggesting that JC hardly affects the RESs contribution to the GC-HRES. Both the algorithms with JC have a REF value of 0,405 despite having different component configurations. The optimal REF values for NSGA-II are higher than MOPSO in Table 4, but the average REF for MOPSO is higher in Table 3.

In Table 3, NSGA-II performed better in minimising COE and LPSP, highlighting its ability to effectively balance cost and reliability, particularly when JC is a priority.

The inclusion of JC led to an increase in the average LPSP for both algorithms. As shown in Table 3, the LPSP for MOPSO increased from 0,015 to 0,027 and the LPSP for NSGA-II increased from 0,000 to 0,010. Thus, configurations prioritising JC slightly compromise on reliability to balance economic and social objectives. In Table 4 LPSP also increases when JC is added for both algorithms. The LPSP for MOPSO increases from 0,000 to 0,031 and the LPSP for NSGA-II increases from 0,003 to 0,014, emphasising that configurations favouring JC are less reliable. The increase in LPSP is smaller for NSGA-II than for MOPSO, reinforcing that NSGA-II is better at finding configurations that balance reliability with other objectives.

The inclusion of JC slightly impacts the average COE for both algorithms. NSGA-II achieved lower average values than MOPSO in both cases, suggesting that it favours lower-cost configurations with fewer components.

Table 4 shows that the inclusion of JC resulted in a higher optimal COE for MOPSO. The COE values increased from 0,031 to 0,051, which indicates that MOPSO increases the components to maximise JC at 4,234. Without JC, MOPSO produced a configuration with only 41 PVs. With JC, the configuration changed to 40 PVs, 1 WT and 19 Bats, resulting in 41 RESs from 60 total components, corresponding to an increase in REF.

In contrast, in Table 4, NSGA-II achieved a higher optimal JC at 4,492 with a lower optimal COE. The COE values increased from 0,046 to 0,041, suggesting that NSGA-II favours configurations that balance JC with lower COE by selecting a mix of components that are both cost-effective and capable of generating jobs. The total components were reduced from 54 components (53 are RESs) to 49 components (46 are RESs). The PVs and Bats increased while the WTs decreased. PVs create almost double the jobs created by WT. Hence, NSGA-II favours a configuration with more PVs when JC is included.

The NPC increased from 1853748 to 2864127 when JC was added to MOPSO in Table 4. This indicates the need for increased investment in components for the GC-HRES to create employment. *NSGA-II with JC* has a lower NPC at 2343234 in Table 4. This suggests that NSGA-II manages to create employment with a more economical setup.

The GHG values for MOPSO decreased significantly from 565211 to 546685 in Table 4 after the introduction of JC in the MOO, possibly due to a more diverse configuration that included Bats and WTs. This configuration reduced dependence on the grid, thereby lowering GHG emissions. The GHG values for NSGA-II increased when JC was added to the MOO from 538602 to 548649 in Table 4 due to the increase in the number of PVs. The increase in the number of PVs created more jobs but also produced more GHG emissions than WTs. The GHG produced by both algorithms with JC is comparable despite the difference in component configuration.

Figures 4, 5 and 6 provide a clearer picture of how compromises between technical, economic, environmental, and social objectives are achieved in each test case.

From the heatmap in Figure 4, itNSGA-II without JC appears to be most reliable configuration, achieving the lowest actual LPSP and thus the highest normalised value of 1.000 in the heatmap. It is important to reiterate that the values for LPSP and COE were inverted, as they are minimisation objectives, to ensure that higher values represent better performance. Consequently, a high value for LPSP on the heatmap corresponds to an actual low value for LPSP as seen in Table 3.

In contrast, *MOPSO with JC* registers the highest normalised LPSP of 0.000, indicating a marked compromise in reliability when JC is prioritised. *MOPSO with JC* excels environmentally and socially, attaining the highest REF and JC values at 1.000. This demonstrates how MOPSO emphasises maximising renewable energy integration and employment potential. *NSGA-II with JC* offers a more balanced solution, with a high JC value of 0.721 and moderate values for other objectives.

From an economic perspective, *NSGA-II with JC* achieves the lowest actual COE, shown as the highest normalised value of 1.000. This confirms its strength in cost efficiency even when a fourth social objective is introduced. In contrast, *MOPSO with JC* has the highest normalised COE of 0.000, highlighting the economic cost of prioritising social and environmental goals.

All axes in the radar graph in Figure 5 have been normalised, scaled and inverted so that higher values represent more desirable results for all objectives. This uniform format simplifies the comparison of the strengths and weaknesses of each test case.

The *NSGA-II with JC* test case forms a well-rounded shape, indicating a balanced compromise in all objectives. It has moderate to high normalised values across all objectives. It excels in COE and JC while maintaining moderate performance in REF and LPSP. This reinforces the effectiveness of NSGA-II in producing balanced solutions.

In contrast, *MOPSO with JC* displays a bias toward REF and JC. This reflects its focus on environmental and social benefits, but exhibits a lower performance in COE and LPSP. This reinforces the trends observed in the heatmap in Figure 4, where the social-environmental preference of *MOPSO with JC* came at the cost of reliability and economic feasibility.

The *Original Study* and *Replicated MOPSO* test cases, which exclude JC as an objective, display moderate performance in the technical and economic objectives of LPSP and COE. They have a relatively lower performance in REF with no social benefit. The narrow radar profiles of these test cases highlight their limited objective scope.

NSGA-II without JC prioritises reliability and cost by achieving the highest LPSP and COE, indicating that it provides the most cost-effective and reliable configuration when social objectives are excluded. However, the lack of social and environmental benefits limits its holistic feasibility with respect to larger sustainability goals. Figure 5 perfectly illustrates how the inclusion of JC as a fourth objective reshapes the MOO outcomes.

In Figure 6, where the normalised values for the minimisation objectives and the variables NPC and GHG were inverted, *NSGA-II with JC* has the highest JC value of 1.000, together with strong values of COE and NPC, at 0.667 and 0.676, respectively. It has moderate reliability with LPSP at 0.548 but also has one of the lowest REF values at 0.122 which is directly related to poor performance in GHG emission reduction at 0.333. This test case reflects compromises between social and economic benefits with reasonable reliability at the cost of environmental benefits.

In contrast, *MOPSO with JC* has the lowest reliability with an LPSP of 0.000 and a modest performance in COE at 0.333 and NPC at 0.360. It also achieves REF and GHG values of 0.122 and 0.372, respectively, which are comparable to the values achieved by NSGA-II. However, *MOPSO with JC* has a high JC value of 0.943. This shows the compromise introduced by prioritising JC, which results in relatively low values in all other variables.

The *Original Study* and *Replicated MOPSO* test cases have excellent reliability as both have the highest normalised LPSP at 1.000. They also show strong economic performance, with COE values of 0.967 and 1.000, respectively. This correlates with their high NPC values of 1.000 and 0.973, respectively. However, both cases perform poorly in REF and GHG, indicating limited integration of renewable energy and insufficient environmental benefits.

The stacked bar graph in Figure 7 reveals clear shifts in GC-HRES design priorities depending on the MOO set-up.

The configurations from the *Original Study* and *Replicated MOPSO* consist solely of PV panels, 40 and 41 units, respectively, which is indicative of an overreliance on a single RES and no storage capacity. The simplicity of this GC-HRES configuration correlates with economic efficiency but limits flexibility of the system and environmental benefits.

The inclusion of JC as an objective in MOPSO results in a more diverse configuration with 1 WT and 19 Bats alongside 40 PVs. This shift reflects the attempt of MOPSO to increase employment potential by integrating more components, especially components with larger JC factors.

The NSGA-II configurations show distinctly diverse configurations, particularly in the inclusion of WTs. In particular, NSGA-II without JC includes the highest number of WTs at 23, emphasising its strategy to balance reliability and cost. When JC is included, the NSGA-II reduces WTs and slightly increases PVs and Bats, reflecting a shift toward components that create more jobs, such as PVs, while maintaining a cost-effective structure.

The MOPSO approach of incremental optimisation led to configurations with more components, especially Bats, when JC was included in the MOO. This resulted in an improved REF and reduced GHG emissions due to less dependence on the grid. However, this came at the expense of increased COE and NPC.

In contrast, NSGA-II was more flexible in balancing objectives, often favouring configurations with fewer but more diverse components. When JC was added to the MOO, NSGA-II reduced the RES components by increasing PVs at the cost of increasing the GHG emission as seen in Table 4. Thus, NSGA-II was cost-effective while also having competitive JC values.

The reshaping of the Pareto front with the inclusion of JC highlights the complexity introduced by the additional objective. For both algorithms, the expanded Pareto front produced more diverse solutions as a result of the varied compromises between LPSP, REF, COE, and JC.

In general, solutions from MOPSO prioritised social and environmental benefits, while NSGA-II excelled in the optimisation of cost and reliability while maintaining respectable JC and REF values. This dichotomy suggests that priorities such as maximising social impact with MOPSO or achieving balanced, cost-effective configurations with NSGA-II must be weighed in accordance with the underlying purpose of the GC-HRES.

Consequently, NSGA-II would be the preferred choice for balanced optimisation, achieving lower costs and greater reliability alongside competitive social benefits. Alternatively, MOPSO excels in scenarios where maximising REF and JC are paramount. The inclusion of JC introduces nuanced compromises between objectives, enriching the solution space, and offering greater flexibility in adjusting the GC-HRES design with broader socio-economic and environmental objectives.

B. COMPARISON OF MOPSO AND NSGA-II IN TERMS OF DIVERSITY

NSGA-II consistently outperforms MOPSO in maintaining solution diversity due to differences in exploration and exploitation strategies along with diversity and preservation mechanisms.

NSGA-II uses crowding distance to prioritise diversity during selection, favouring less crowded solutions in the objective space, thus ensuring a well-distributed set of solutions across the Pareto front. Additionally, crossover and mutation operators enable the broad exploration of the solution space, promoting diversity by generating varied solutions [44], [45]. The emphasis on exploration is evident in the component configurations produced by NSGA-II, as shown in Table 4.

In contrast, MOPSO relies on particle velocity and position updates, guided by leaders selected from the repository. These leaders dictate the "trend" for subsequent particles, often leading to a concentrated search in specific regions of the solution space. While this strategy facilitates the exploitation of promising areas within the solution space, it also reduces diversity across generations [43]. Another factor is repository management in MOPSO. Poorly managed repositories can result in stored solutions being too similar, thereby limiting diversity. Subsequent repository particles are guided by "repository leaders". This guidance could create a bias which could narrow the search space further [43].

The non-dominated sorting and crowding distance mechanisms of NSGA-II ensure diversity preservation across generations. Combined with its evolutionary operators, NSGA-II maintains a well-distributed Pareto front. In comparison, the MOPSO swarm-based approach heavily relies on "follow the leader" dynamics and thus struggles to achieve the same level of diversity.

C. THE LIMITATIONS OF JC FACTORS AND FUTURE WORK

While incorporating JC as an objective expanded the Pareto front, its effectiveness is constrained by the accuracy and context of JC factors. These factors are significantly influenced by assumptions made during data collection, particularly in the manufacturing phase.

The manufacturing of RES components, whether domestically or abroad, directly impacts the local employment potential. While installation and O&M jobs are inherently local, manufacturing processes often involve imported components or systems. The extent of foreign manufacturing of RESs reduces the local employment contribution, but sufficient context-specific information about this phase is scarce [39].

Recursive referencing, the re-use of JC factors from previous publications without context, in studies related to employment potential is common. Thus, the results related to the employment potential of RES components in certain regions or configurations are misleading.

Furthermore, comparing JC factors between studies is challenging due to significant variations in methodologies, assumptions, and regional contexts. The lack of standardisation in data collection and reporting further complicates these comparisons [39].

Future research should prioritise the collection of comprehensive and updated primary data on job creation across all three RES deployment phases from diverse geographic regions. There should also be a focus on establishing standardised indicators and transparent methodologies to measure and report JC factors. Enhanced clarity on how employment potential evolves with experience, scale, and technological advancements is critical [39].

Beyond JC, future studies should explore alternative social objectives such as social acceptability, land use, and impacts on productivity, efficiency, and quality of life associated with implementing GC-HRESs. These considerations could provide a broader perspective on the societal impacts of RES deployment.

D. IMPACT OF CHANGING THE BATTERY CONSTRAINT

The results of the test cases in Table 4 show some impractical configurations. Functioning GC-HRESs typically require a battery storage system. The configurations that were produced by the *Original Study* and *Replicated MOPSO* test cases when the MOO did not integrate JC, did not have battery banks in the optimal GC-HRES configuration. However, when JC was included in the MOO, MOPSO produced configurations that included PV panels, wind turbines, and batteries. In particular, NSGA-II consistently generated diverse configurations with or without JC, reflecting its ability to maintain practical GC-HRES designs under varying objectives.

The feasibility of a GC-HRES configuration should not depend on the inclusion of specific objectives. Thus, the search space was modified by changing the battery bank constraint from 0 to 100 to 1 to 100, ensuring that there was at least one battery bank in all configurations. MOPSO was then re-evaluated under the revised constraint using three objectives: LPSP, COE, and REF. The results are summarised in *Battery Constraint MOPSO* in Table 4 and Figure 6.

The modified battery bank constraint ensured that MOPSO produced practical configurations, even without JC as an objective. The modified constraint led to a significant increase in component diversity from a configuration with 41 PVs to a configuration with 28 PVs, 35 WTs, and 5 Bats, as shown in Table 4 and Figure 7.

Previously, solutions with zero batteries were possible, and these solutions would dominate because they performed well with respect to the other objectives, such as improving reliability (LPSP) and increasing the contribution of renewable energy (REF). When such dominant solutions were present, MOPSO favoured them as repository leaders, narrowing the search space and reducing diversity [43]. Thus, the bias toward the zero battery solution was eliminated.

MOPSO was compelled to explore configurations that included at least one battery, thereby broadening the search space by reducing the convergence toward narrow solution regions and encouraging the exploration of previously under-searched areas, leading to greater solution diversity.

In Figure 6, the Battery Constraint MOPSO test case achieves the highest REF and GHG values at 1.000, clearly illustrating the benefit of enforced battery inclusion in GC-HRES to improve environmental performance. However, this test case also yields the lowest COE and NPC at 0.000, highlighting its significant investment burden and high cost to generated energy ratio, likely due to component diversity. This diversity is shown in the stacked bar graph in Figure 7, where the test case produces the most diverse and component-heavy GC-HRES configuration from the rest. This outcome highlights how altering the search space, by enforcing at least one battery, leads to more practical solutions with improved storage capacity and environmental performance.

E. COMPUTATION TIME

The MOO frameworks were implemented and evaluated using the open source Keras Python library, using efficient numerical computations with the TensorFlow backend in Google Colaboratory, a hosted Jupyter notebook service that executes Python code in a browser environment [55]. The development, testing and evaluation were performed locally on an Aspire A315-53 laptop with the following specifications: a processor (CPU) of Intel(R) Core(TM) i5-7200U, an installed RAM of 4 GB DDR4, of which 3,88 GB is usable, and a storage of 1 TB HDD with an effective storage of 930 GB. The computation time for each test case in this environment was recorded in Table 5. The inclusion of JC in the MOPSO algorithm had a negligible impact on the computation time, increasing it by only 4 minutes. Modifying the battery bank constraint resulted in a 2 minute decrease compared to the Replicated MOPSO. The slight decrease in time was due to the narrowing of the search space. Thus, adding an objective or adjusting a decision variable constraint of a decision variable constraint does not significantly affect the MOPSO computation time. A similar trend was observed for the NSGA-II algorithm, where including JC increased the computation time by only 5 minutes. Thus, the introduction of an additional objective causes only a small increase in the NSGA-II computation time.

The MOPSO algorithms consistently have greater computation times than the NSGA-II algorithms. On average, the MOPSO algorithms run approximately 30 minutes longer

TABLE 5. The computation time for each test case.

Algorithm	Computation Time
Replicated MOPSO	2h 1mins
MOPSO with JC	2h 5min
NSGA-II	1h 30min
NSGA-II with JC	1h 35min
Battery Constraint MOPSO	2h 3min

than their NSGA-II counterparts, indicating that NSGA-II is computationally more efficient than MOPSO.

VII. CONCLUSION

This paper introduced a novel MOO framework for a GC-HRES to achieve a design that is technically robust, economically viable, environmentally sustainable, and socially beneficial, by explicitly integrating JC as a social objective, along with traditional technical, economic, and environmental objectives. Previous studies have addressed JC only in post-optimisation analysis or limited its integration in the MOO to off-grid systems. This study positions JC as a core optimisation objective, in which the optimisation problem aimed to minimise LPSP and COE, while maximising REF and JC. Metaheuristic algorithms, MOPSO and NSGA-II, were used to optimise the number of solar panels, wind turbines, and battery banks in two cases, one that excluded JC and the other which included JC as the fourth objective.

The integration of JC as an explicit objective expanded the Pareto front, which led to new compromises between objectives, thereby increasing the diversity of the solution space. MOPSO effectively explored this broader space and favoured configurations that maximise REF and JC. In contrast, NSGA-II showed superior diversity preservation because of its crowding-distance operator and evolutionary mechanisms, achieving a computationally efficient balance across objectives. NSGA-II produced balanced solutions with lower LPSP and COE, while still achieving competitive JC and REF outcomes. Although NSGA-II is the preferred algorithm for generating balanced, cost-effective, reliable configurations with reasonable social benefits, MOPSO remains advantageous when environmental and social priorities, particularly JC, take precedence.

As a proof of concept, the proposed MOO framework was based on a case study. However, the framework is designed to be adaptable with an integrated structure. Input parameters such as solar and wind profiles, energy demand, and component costs can be easily modified for different geographical or economic contexts. Similarly, objective functions can be redefined or expanded to include additional social goals or even other technical, economic, and environmental targets. The constraints on the decision variable ranges and objective function limits can be adjusted to the requirements of the energy system that is being optimised. The chosen metaheuristic algorithms, MOPSO and NSGA-II, are robust to changes in dimensionality and complexity, making them appropriate for optimising both small-scale microgrids and larger urban or national-level energy systems. For example, the proposed MOO framework could be adapted to urban settings with dynamic electricity pricing adjustments throughout the day, alongside demand response initiatives, or to policy-oriented environments that include carbon pricing or renewable energy subsidies. This transferability supports the claim that the proposed framework is replicable and adaptable.

This study demonstrated that the integration of JC as an explicit objective in the MOO fostered a more holistic approach to GC-HRES design, aligning social benefits with technical, economic, and environmental goals. This approach improved the practical feasibility of GC-HRES configurations while supporting broader sustainability transitions. The proposed framework is replicable and adaptable and thus lays the groundwork for future research on the integration of social indicators into GC-HRES design optimisation.

APPENDIX A
BATTERY STORAGE SYSTEM CONSTRAINTS

The excess energy from the GC-HRES is stored in the battery storage bank and can be used when RESs are fail to meet the load demand. The energy storage capacity of the battery adheres to the restrictions shown in (27), (28) and (29) [31]:

$$E_{Bat,min} \leq E_{Bat}(t) \leq E_{Bat,max} \tag{27}$$

$$E_{Bat,max} = E_{Bat,cap} \tag{28}$$

$$E_{Bat,min} = E_{Bat,max}(1 - DOD) \tag{29}$$

where E_{Bat} is the battery bank nominal capacity (kWh), $E_{Bat,min}$ is the minimum allowable storage battery capacity (kWh), $E_{Bat,max}$ is the maximum allowable storage battery capacity (kWh), $E_{Bat,cap}$ is the battery storage capacity (kWh) and DOD is the depth of discharge, taken as 80% [31]. DOD is the percentage or fraction of the capacity that has been removed from a fully charged battery [56].

APPENDIX B
NET PRESENT COST, GREENHOUSE GAS EMISSIONS AND SYSTEM CONSTRAINTS CALCULATIONS

A. NET PRESENT COST OF THE COMPONENTS

The NPC of the PV system, NPC_{pv} is calculated through [5]:

$$\begin{aligned} NPC_{pv} &= IC_{pv} + O\&MC_{pv} \\ &= N_{pv} \times \left[IPR_{pv} + \sum_{n=0}^{25} \frac{OMP_{pv}}{(1 + \frac{I_r - I_f}{1+I_f})^{n-1}} \right] \end{aligned} \tag{30}$$

where NPC_{pv} is the NPC of the PV system (\$), IC_{pv} is the initial cost of the PV panels (\$), $O\&MC_{pv}$ is the operation and maintenance (O&M) cost of the panels (\$), N_{pv} is the number of PV modules, IPR_{pv} is the initial price of PV system (\$) and OMP_{pv} is the O&M price of PV system (\$), I_r is the interest rate and I_f is the inflation [5]. As the lifetimes of the PV system and the project are both 25 years, there is no replacement cost for the duration of the project, and therefore the replacement cost is zero [5]. This study assumed that the capital cost of the 30kW PV panel would be \$42 000 with an 0&M cost of \$40 per panel [5].

The NPC of the wind turbine, NPC_{WT} is calculated as follows [5]:

$$NPC_{WT} = IC_{WT} + RC_{WT} + O\&MC_{WT} = N_{WT} \times \left[IPR_{WT} + \frac{RP_{WT}}{(1+\frac{I_r - I_f}{1+I_f})^{15}} + \sum_{n=0}^{25} \frac{OMP_{WT}}{(1+\frac{I_r - I_f}{1+I_f})^{n-1}} \right] \tag{31}$$

where NPC_{WT} is the NPC of the wind turbine (\$), IPR_{WT} is the initial price of wind turbines (\$), OMP_{WT} is the O&M price of wind turbines (\$), N_{WT} is the number of wind turbines, IC_{WT} is the initial capital cost of the wind turbine (\$), $O\&MC_{WT}$ is the O&M costs of the wind turbine (\$) and RP_{WT} is the replacement price of wind turbine (\$) [5]. This study assumed that the capital cost of the 50kW wind turbine was \$50 000 with a replacement cost of \$25 000 and an O&M cost of \$75 per wind turbine [5].

The NPC of the battery, NPC_{BAT} can be calculated as shown below [5]:

$$NPC_{BAT} = IC_{BAT} + O\&MC_{BAT} = N_{BAT} \times \left[IPR_{BAT} + \sum_{n=0}^{25} \frac{OMP_{BAT}}{(1+\frac{I_r - I_f}{1+I_f})^{n-1}} \right] \tag{32}$$

where NPC_{BAT} is the NPC of the battery (\$), IPR_{BAT} is the initial price of a battery bank (\$), OMP_{BAT} is the O&M price of the battery bank (\$), N_{BAT} is the number of battery banks, IC_{BAT} is the initial capital cost of the battery (\$), $O\&MC_{BAT}$ is the O&M cost of the battery (\$) [5]. As the lifetimes of the Bat and the project are both 25 years, there is no replacement cost for the duration of the project, and therefore the replacement cost is zero [5]. This study assumed that the capital cost of the 1000 Ah Nickel Iron Battery was \$42 250 with an O&M cost of \$5 per battery bank [5].

B. GREENHOUSE GAS EMISSIONS

The Greenhouse Gas (GHG) emissions from the grid can be calculated from (33) [5]:

$$\begin{aligned} &Grid\ GHG\ emissions \\ &= Total\ load\ supplied\ by\ the\ grid\ \times Grid_{ef} \times GWP \end{aligned} \tag{33}$$

where $Grid_{ef}$ $(kgCO2/kWh)$ is the electricity-specific factor particular to each country. For the GC-HRES under consideration, this value was assumed to be 0.500886 $(kgCO2/kWh)$ for Egypt [5], [57]. GWP is the Global Warming Potential, which measures how much a particular GHG impacts global warming compared to carbon dioxide (CO_2). CO_2 is used as a reference point from which the emissions of different GHGs are compared. CO_2 has a GWP of 1 and the other GHGs listed in the Kyoto Protocol all have higher GWPs compared to CO_2 [58]. Methane (CH_4), nitrous oxide (N_2O) and sulfur hexafluoride (SF_6) have a GWP of 21, 310 and 23,900, respectively, as referenced by the International Panel on Climate Change (IPCC), Fifth Assessment Report, 2014 (AR5) [5], [59].

The GHG emissions associated with the PV system can be calculated using (34) [5]:

$$E_{mPV} = \sum_{t=1}^{8760} P_{PV}(t) \times e_{pv} \times GWP \tag{34}$$

where P_{PV} (kWh) is the annual power produced by the PV system and e_{pv} $(kgCO2 - eq/kWh)$ is the emission factor of the PV system, chosen to be 0.045 $(kgCO2 - eq/kWh)$ for a mono-Si PV in the GC-HRES [5], [60].

The GHG emissions from the WT system can be calculated using (35) [5]:

$$E_{mWT} = \sum_{t=1}^{8760} P_{WT}(t) \times e_{WT} \times GWP \tag{35}$$

where P_{WT} (kWh) is the annual power produced by the WT system and e_{WT} $((kgCO2 - eq/kWh)$ is the emission factor of the WT system which was chosen to be 0.011 $(kgCO2 - eq/kWh)$ for the GC-HRES in this study [5], [61].

It then follows that the total GHG emissions produced by the GC-HRES can be summed as (36) [5]:

$$System_{GHG_total} = PV_{GHG} + WT_{GHG} + Grid_{GHG} \tag{36}$$

To calculate the net savings of GHG emissions due to the implementation of the GC-HRES, a base case calculation is required for comparison. In this study, the base case was assumed to be the scenario in which only the grid was used to meet the load demand of the village.

The base case GHG emissions can be calculated as follows in (37) [5]:

$$Base\ Case\ GHG\ emissions = Total\ load\ \times Grid_{ef} \times GWP \tag{37}$$

After which, the net savings in GHG emissions can be calculated in (38) [5]:

$$net_{savingGHG} = BaseCase_{GHG} - SystemGHG_total \tag{38}$$

C. CONSTRAINTS

1) DECISION VARIABLE BOUNDARY

This relationship is illustrated by (39) [5]:

$$N_x^{min} \le N_x \le N_x^{max}, x\epsilon\{PV, WT, BAT\} \tag{39}$$

where N_x is the number of component x [5].

2) BATTERY STORAGE LIMITS

The storage capacity of the battery and hence available battery energy has the following limits as shown in (40) [31]:

$$E_{Bat,min} \le E_{Bat}(t) \le E_{Bat,max} \tag{40}$$

3) ENERGY BALANCE

The sum of the energy generated by all the online units must be equal the system load demand over the entire scheduling time range. For the system hourly load demand and the hourly energy generation, the energy balance is illustrated in (41) [5]:

$$E_{PV}(t) + E_{WT}(t) \pm E_{grid}(t) \pm EBat(t)$$
$$-E_{dump}(t) \geq \frac{E_{load}(t)}{\eta_{inv}} \tag{41}$$

where E_{PV}: PV generator energy, E_{WT} is the WT generator energy, $\pm EBat$: energy supplied and used by the battery, $\pm E_{grid}$: energy bought and sold to the grid, E_{dump} is the energy wasted due to excessive grid and load unavailability, η_{inv}inverter efficiency of 0,9 [5].

REFERENCES

[1] J. D. Fonseca, J.-M. Commenge, M. Camargo, L. Falk, and I. D. Gil, "Sustainability analysis for the design of distributed energy systems: A multi-objective optimization approach," *Appl. Energy*, vol. 290, pp. 1–20, May 2021, doi: 10.1016/j.apenergy.2021.116746.

[2] E. L. V. Eriksson and E. M. Gray, "Optimization of renewable hybrid energy systems—A multi-objective approach," *Renew. Energy*, vol. 133, pp. 971–999, Apr. 2019, doi: 10.1016/j.renene.2018.10.053.

[3] Y. He, S. Guo, P. Dong, Y. Zhang, J. Huang, and J. Zhou, "A state-of-the-art review and bibliometric analysis on the sizing optimization of off-grid hybrid renewable energy systems," *Renew. Sustain. Energy Rev.*, vol. 183, pp. 1–26, Sep. 2023, doi: 10.1016/j.rser.2023.113476.

[4] O. Nadjemi, T. Nacer, A. Hamidat, and H. Salhi, "Optimal hybrid PV/wind energy system sizing: Application of cuckoo search algorithm for Algerian dairy farms," *Renew. Sustain. Energy Rev.*, vol. 70, pp. 1352–1365, Apr. 2017, doi: 10.1016/j.rser.2016.12.038.

[5] S. Barakat, H. Ibrahim, and A. A. Elbaset, "Multi-objective optimization of grid-connected PV-wind hybrid system considering reliability, cost, and environmental aspects," *Sustain. Cities Soc.*, vol. 60, pp. 1–13, Sep. 2020, doi: 10.1016/j.scs.2020.102178.

[6] A. Chauhan and R. P. Saini, "Techno-economic feasibility study on integrated renewable energy system for an isolated community of India," *Renew. Sustain. Energy Rev.*, vol. 59, pp. 388–405, Jun. 2016, doi: 10.1016/j.rser.2015.12.290.

[7] J. Lian, Y. Zhang, C. Ma, Y. Yang, and E. Chaima, "A review on recent sizing methodologies of hybrid renewable energy systems," *Energy Convers. Manage.*, vol. 199, pp. 1–23, Nov. 2019, doi: 10.1016/j.enconman.2019.112027.

[8] Z. Zhang, H. Liao, and A. Tang, "Renewable energy portfolio optimization with public participation under uncertainty: A hybrid multi-attribute multi-objective decision-making method," *Appl. Energy*, vol. 307, Feb. 2022, Art. no. 118267, doi: 10.1016/j.apenergy.2021.118267.

[9] M. A. Cuesta, T. Castillo-Calzadilla, and C. E. Borges, "A critical analysis on hybrid renewable energy modeling tools: An emerging opportunity to include social indicators to optimise systems in small communities," *Renew. Sustain. Energy Rev.*, vol. 122, Apr. 2020, Art. no. 109691, doi: 10.1016/j.rser.2019.109691.

[10] M. Farghali, A. I. Osman, Z. Chen, A. Abdelhaleem, I. Ihara, I. M. A. Mohamed, P.-S. Yap, and D. W. Rooney, "Social, environmental, and economic consequences of integrating renewable energies in the electricity sector: A review," *Environ. Chem. Lett.*, vol. 21, no. 3, pp. 1381–1418, Jun. 2023, doi: 10.1007/s10311-023-01587-1.

[11] A. Giedraityte, S. Rimkevicius, M. Marciukaitis, V. Radziukynas, and R. Bakas, "Hybrid renewable energy systems—A review of optimization approaches and future challenges," *Appl. Sci.*, vol. 15, no. 4, p. 1744, Feb. 2025, doi: 10.3390/app15041744.

[12] S. Proença and P. Fortes, "The social face of renewables: Econometric analysis of the relationship between renewables and employment," *Energy Rep.*, vol. 6, pp. 581–586, Feb. 2020, doi: 10.1016/j.egyr.2019.09.029.

[13] E. Llera Sastresa, A. A. Usón, I. Z. Bribián, and S. Scarpellini, "Local impact of renewables on employment: Assessment methodology and case study," *Renew. Sustain. Energy Rev.*, vol. 14, no. 2, pp. 679–690, Feb. 2010, doi: 10.1016/j.rser.2009.10.017.

[14] S. Habibzadeh, F. R. Astaraei, and M. H. Jahangir, "Sustainability assessment of a petrochemical plant electricity supply based on 4E optimization of various hybrid renewable energy systems scenarios," *Energy Convers. Manage.*, vol. 325, Feb. 2025, Art. no. 119357, doi: 10.1016/j.enconman.2024.119357.

[15] M. Yalılı, T. Menlik, and F. E. Boran, "A novel multi-objective decision-making model to determine optimum resource and capacity configuration for hybrid electricity generation systems: A comparative case study in Türkiye," *Appl. Energy*, vol. 376, Dec. 2024, Art. no. 124338, doi: 10.1016/j.apenergy.2024.124338.

[16] M. Ram, A. Aghahosseini, and C. Breyer, "Job creation during the global energy transition towards 100% renewable power system by 2050," *Technol. Forecasting Social Change*, vol. 151, Feb. 2020, Art. no. 119682, doi: 10.1016/j.techfore.2019.06.008.

[17] R. Hassan, B. K. Das, and M. Hasan, "Integrated off-grid hybrid renewable energy system optimization based on economic, environmental, and social indicators for sustainable development," *Energy*, vol. 250, Jul. 2022, Art. no. 123823, doi: 10.1016/j.energy.2022.123823.

[18] P. Singh, M. Pandit, and L. Srivastava, "Techno-socio-economic-environmental estimation of hybrid renewable energy system using two-phase swarm-evolutionary algorithm," *Sustain. Energy Technol. Assessments*, vol. 53, Oct. 2022, Art. no. 102483, doi: 10.1016/j.seta.2022.102483.

[19] P. Das, B. K. Das, M. Rahman, and R. Hassan, "Evaluating the prospect of utilizing excess energy and creating employments from a hybrid energy system meeting electricity and freshwater demands using multi-objective evolutionary algorithms," *Proc. Energy*, vol. 238, Jan. 2021, Art. no. 121860, doi: 10.1016/j.energy.2021.121860.

[20] Y. Sawle, S. C. Gupta, and A. K. Bohre, "Socio-techno-economic design of hybrid renewable energy system using optimization techniques," *Renew. Energy*, vol. 119, pp. 459–472, Apr. 2018, doi: 10.1016/j.renene.2017.11.058.

[21] P. K. Kushwaha, P. Ray, and C. Bhattacharjee, "Optimal sizing of a hybrid renewable energy system: A socio-techno-economic-environmental perspective," *J. Sol. Energy Eng.*, vol. 145, no. 3, pp. 1–19, Jun. 2023, doi: 10.1115/1.4055196.

[22] P. K. Kushwaha and C. Bhattacharjee, "Socio-techno-economic-environmental sizing of hybrid renewable energy system using metaheuristic optimization approaches," *Environ. Prog. Sustain. Energy*, vol. 43, no. 3, pp. 1–19, Mar. 2024, doi: 10.1002/ep.14386.

[23] T. Al Shidhani, A. Ioannou, and G. Falcone, "Multi-objective optimisation for power system planning integrating sustainability indicators," *Energies*, vol. 13, no. 9, pp. 1–32, May 2020.

[24] M. R. Elkadeem, K. M. Kotb, M. A. Abido, H. M. Hasanien, E. G. Atiya, D. Almakhles, and M. F. Elmorshedy, "Techno-enviro-socio-economic design and finite set model predictive current control of a grid-connected large-scale hybrid solar/wind energy system: A case study of sokhna industrial zone, Egypt," *Energy*, vol. 289, Feb. 2024, Art. no. 129816, doi: 10.1016/j.energy.2023.129816.

[25] E. Uyan, "Tecno-econo-enviro-social assessment of clean electrification for a marine equipment manufacturing plant in Türkiye through hybrid renewable energy system with demand response," *Energy*, vol. 304, Mar. 2024, Art. no. 132015, doi: 10.1016/j.energy.2024.132015.

[26] M. A. Abdoulaye, S. Waita, C. W. Wekesa, and J. M. Mwabora, "Optimal sizing of an off-grid and grid-connected hybrid photovoltaic-wind system with battery and fuel cell storage system: A techno-economic, environmental, and social assessment," *Appl. Energy*, vol. 365, Jul. 2024, Art. no. 123201, doi: 10.1016/j.apenergy.2024.123201.

[27] M. B. Eteiba, S. Barakat, M. M. Samy, and W. I. Wahba, "Optimization of an off-grid PV/biomass hybrid system with different battery technologies," *Sustain. Cities Soc.*, vol. 40, pp. 713–727, Jul. 2018.

[28] J. A. Duffie and W. A. Beckman, *Solar Engineering of Thermal Processes*. Hoboken, NJ, USA: Wiley, 2013.

[29] S. M. Hakimi, S. M. M. Tafreshi, and A. Kashefi, "Unit sizing of a stand-alone hybrid power system using particle swarm optimization (PSO)," in *Proc. IEEE Int. Conf. Autom. Logistics*, Aug. 2007, pp. 3107–3112.

[30] A. Malheiro, P. M. Castro, R. M. Lima, and A. Estanqueiro, "Integrated sizing and scheduling of wind/PV/diesel/battery isolated systems," *Renew. Energy*, vol. 83, pp. 646–657, Nov. 2015.

[31] A. Elbaz and M. T. Guneser, "Multi-objective optimization method for proper configuration of grid-connected PV-wind hybrid system in terms of ecological effects, outlay, and reliability," *J. Electr. Eng. Technol.*, vol. 16, no. 2, pp. 771–782, Mar. 2021, doi: 10.1007/s42835-020-00635-y.

[32] S. Diaf, D. Diaf, M. Belhamel, M. Haddadi, and A. Louche, "A methodology for optimal sizing of autonomous hybrid PV/wind system," *Energy Policy*, vol. 35, no. 11, pp. 5708–5718, Nov. 2007, doi: 10.1016/j.enpol.2007.06.020.

[33] A. K. Kaviani, H. R. Baghaee, and G. H. Riahy, "Optimal sizing of a stand-alone wind/photovoltaic generation unit using particle swarm optimization," *Simulation*, vol. 85, no. 2, pp. 89–99, Feb. 2009, doi: 10.1177/0037549708101181.

[34] S. Nomura, Y. Ohata, T. Hagita, H. Tsutsui, S. Tsuji-Iio, and R. Shimada, "Wind farms linked by SMES systems," *IEEE Trans. Appiled Supercond.*, vol. 15, no. 2, pp. 1951–1954, Jun. 2005, doi: 10.1109/TASC.2005.849343.

[35] A. H. Fathima and K. Palanisamy, "Optimization in microgrids with hybrid energy systems—A review," *Renew. Sustain. Energy Rev.*, vol. 45, pp. 431–446, May 2015, doi: 10.1016/j.rser.2015.01.059.

[36] R. Luna-Rubio, M. Trejo-Perea, D. Vargas-Vázquez, and G. J. Ríos-Moreno, "Optimal sizing of renewable hybrids energy systems: A review of methodologies," *Sol. Energy*, vol. 86, no. 4, pp. 1077–1088, Apr. 2012.

[37] C. B. Egypt. *Monthly Interest Rates*. Accessed: May 12, 2025. [Online]. Available: https://www.cbe.org.eg/en/economic-research/statistics/monthly-interest-rates

[38] *Irena Working Paper: Renewable Energy Jobs: Status, Prospects & Policies*, IRENA, Abu Dhabi, UAE, 2011.

[39] L. Cameron and B. van der Zwaan, "Employment factors for wind and solar energy technologies: A literature review," *Renew. Sustain. Energy Rev.*, vol. 45, pp. 160–172, May 2015, doi: 10.1016/j.rser.2015.01.001.

[40] D. M. Kammen, K. Kapadia, and M. Fripp, "Putting renewables to work: How many jobs can the clean energy industry generate? (rael report)," Renewable & Appropriate Energy Lab., Univ. California, Berkeley, CA, USA, 2004.

[41] M. Wei, S. Patadia, and D. M. Kammen, "Putting renewables and energy efficiency to work: How many jobs can the clean energy industry generate in the U.S.?" *Energy Policy*, vol. 38, no. 2, pp. 919–931, Feb. 2010.

[42] H. Ren, Y. Lu, Q. Wu, X. Yang, and A. Zhou, "Multi-objective optimization of a hybrid distributed energy system using NSGA-II algorithm," *Frontiers Energy*, vol. 12, no. 4, pp. 518–528, Dec. 2018, doi: 10.1007/s11708-018-0594-7.

[43] J. Kennedy, "Particle swarm optimization," in *Encyclopedia of Machine Learning*. Boston, MA, USA: Springer, 2011, pp. 760–766, doi: 10.1007/978-0-387-30164-8_630.

[44] Z. Wang, J. Li, G. P. Rangaiah, and Z. Wu, "Machine learning aided multi-objective optimization and multi-criteria decision making: Framework and two applications in chemical engineering," *Comput. Chem. Eng.*, vol. 165, pp. 1–15, Sep. 2022, doi: 10.1016/j.compchemeng.2022.107945.

[45] K. Deb, A. Pratap, S. Agarwal, and T. Meyarivan, "A fast and elitist multiobjective genetic algorithm: NSGA-II," *IEEE Trans. Evol. Comput.*, vol. 6, no. 2, pp. 182–197, Apr. 2002.

[46] J. Blank and K. Deb, "Pymoo: Multi-objective optimization in Python," *IEEE Access*, vol. 8, pp. 89497–89509, 2020.

[47] T. H. W. Bäck, A. V. Kononova, B. van Stein, H. Wang, K. A. Antonov, R. T. Kalkreuth, J. de Nobel, D. Vermetten, R. de Winter, and F. Ye, "Evolutionary algorithms for parameter optimization—Thirty years later," *Evol. Comput.*, vol. 31, no. 2, pp. 81–122, Jun. 2023.

[48] K. Deb, K. Sindhya, and T. Okabe, "Self-adaptive simulated binary crossover for real-parameter optimization," in *Proc. 9th Annu. Conf. Genetic Evol. Comput.*, NY, NY, USA, Jul. 2007, pp. 1187–1194.

[49] K. Deb and R. B. Agrawal, "Simulated binary crossover for continuous search space," *Complex Syst.*, vol. 9, pp. 115–148, Mar. 1995.

[50] C. A. C. Coello, G. T. Pulido, and M. S. Lechuga, "Handling multiple objectives with particle swarm optimization," *IEEE Trans. Evol. Comput.*, vol. 8, no. 3, pp. 256–279, Jun. 2004.

[51] R. Cheraghi and M. H. Jahangir, "Multi-objective optimization of a hybrid renewable energy system supplying a residential building using NSGA-II and MOPSO algorithms," *Energy Convers. Manage.*, vol. 294, Oct. 2023, Art. no. 117515.

[52] A. Alarcon-Rodriguez, G. Ault, and S. Galloway, "Multi-objective planning of distributed energy resources: A review of the state-of-the-art," *Renew. Sustain. Energy Rev.*, vol. 14, no. 5, pp. 1353–1366, Jun. 2010.

[53] C.-L. Hwang and K. Yoon, *Multiple Attribute Decision Making: Methods and Applications a State-of-the-Art Survey*. Cham, Switzerland: Springer, 1981.

[54] Z. Wang and G. P. Rangaiah, "Application and analysis of methods for selecting an optimal solution from the Pareto-optimal front obtained by multiobjective optimization," *Ind. Eng. Chem. Res.*, vol. 56, no. 2, pp. 560–574, Jan. 2017, doi: 10.1021/acs.iecr.6b03453.

[55] M. Abadi, "TensorFlow: Large-scale machine learning on heterogeneous distributed systems," *Preliminary White Paper*, vol. 9, p. 192, Nov. 2016.

[56] N. Achaiboua, M. Haddadib, and A. Maleka, "Lead acid batteries simulation including experimental validation," *J. Power Sources*, vol. 59, no. 185, pp. 1484–1491, 2008.

[57] M. Brander, A. Sood, C. Wylie, A. Haughton, and J. Lovell, "Technical paperl electricity-specific emission factors for grid electricity," Ecometrica, Tech. Rep., 2011. Accessed: Sep. 21, 2025. [Online]. Available: https://bravenewclimate.com/files/assets/media/pdf/electricity_factors_paper.pdf

[58] S. Solomon, "Working group I contribution to the fourth assessment report of the IPCC," in *Climate Change 2007-the Physical Science Basis*. Cambridge, U.K.: Cambridge Univ. Press, 2007, p. 4.

[59] G. Myhre, D. Shindell, F. Bréon, W. J. Collins, J. S. Fuglestvedt, J. Huang, D. Koch, J. Lamarque, D. E. Lee, B. Mendoza, T. Nakajima, A. Robock, G. Stephens, T. Takemura, and H. Zhang, "Anthropogenic and natural radiative forcing," in *Proc. Climate Change Phys. Sci. Basis*, Jun. 2014, pp. 659–740.

[60] J. Peng, L. Lu, and H. Yang, "Review on life cycle assessment of energy payback and greenhouse gas emission of solar photovoltaic systems," *Renew. Sustain. Energy Rev.*, vol. 19, pp. 255–274, Aug. 2012.

[61] T. Ackermann, G. Andersson, and L. Söder, "Distributed generation: A definition," *Electric Power Syst. Res.*, vol. 57, no. 3, pp. 195–204, 2001.

DHRUTI DHEDA received the B.Sc. (Eng.) and M.Sc. (Eng.) degrees in chemical and metallurgical engineering and the M.Sc. (Eng.) degree (cum laude) in electrical and information engineering from the University of the Witwatersrand, Johannesburg, where she is currently pursuing the Ph.D. degree with the School of Electrical and Information Engineering. Her doctoral research explores the multiple objective optimization of hybrid renewable energy systems using meta-heuristic algorithms. Her research particularly emphasises environmental and social aspects of the implementation of technology and innovation. Her research interests include deep learning algorithms and their application to the environmental conservation, water quality monitoring and wastewater analysis, water footprinting, and carbon nanotubes.

JANDRÉ ALBERTYN received the B.Sc. (Eng.) and M.Sc. degrees in electrical and information engineering from the University of the Witwatersrand, in 2016 and 2023, respectively. His master's degree focused on investigating trends in natural heuristics to find sub-optimal solutions to the traveling salesman problem. His research interests include meta-heuristic algorithms and application of various computational techniques to find optimal solutions to NP-hard problems.

KAYODE ADETUNJI received the master's degree in electrical engineering from the University of Johannesburg, South Africa, in 2018, and the Ph.D. degree from the School of Electrical and Information Engineering, University of the Witwatersrand, in 2022. During his academic journey, he developed optimization algorithms and machine learning techniques, especially reinforcement learning, to improve power systems networks by integrating renewable energy sources, battery

systems, and electric vehicles. His research led to multiple publications in high-impact journals, and he was recognized as a Golden Key member for his outstanding performance. Additionally, he created monitoring systems for various fields, including energy, health, and agriculture. He is currently works with the Multimorbidity in Africa, Digital Innovation, Visualization and Application (MADIVA) research hub with Sydney Brenner Institute for Molecular Bioscience. His current work is focused on developing explainable machine learning models for both single disease and multimorbidity risk prediction, as well as automatic stratification techniques for disease risk screening. His research interests include intuitive machine learning models, optimization algorithms, decision theory and preference aggregation, and health-energy nexus.

ZHENQING LIU received the Ph.D. degree from The University of Tokyo, Japan. He received a national scholarship from Japanese Ministry of Education, Culture, Sports, Science and Technology. He was a Postdoctoral Fellow and a Researcher with The University of Tokyo. After 2015, he was a Lecturer, an Associate Professor, and a Professor (Ph.D. Supervisor) with the School of Civil and Hydraulic Engineering, Huazhong University of Science and Technology. He is currently with the Department of Architectural Engineering, School of Civil and Hydraulic Engineering, Huazhong University of Science and Technology, a Professor, a Doctoral Supervisor, top young talent of the National Ten Thousand Talents Plan, Chutian Scholar (student), Hubei Province, and one of the top 100 postdoctoral candidates in China.

ADNAN M. ABU-MAHFOUZ (Senior Member, IEEE) received the M.Eng. and Ph.D. degrees in computer engineering from the University of Pretoria. He is currently the Center Manager of the Emerging Digital Technologies for 4IR (EDT4IR) Research Centre, Council for Scientific and Industrial Research (CSIR), a Professor Extraordinaire with the Tshwane University of Technology, a Visiting Professor with the University of Johannesburg, and an Extraordinary Faculty Member with the University of Pretoria. He participated in the formulation of many large and multidisciplinary research and development successful proposals (as Principal Investigator or main author/contributor). He is the Founder of the Smart Networks collaboration initiative that aims to develop efficient and secure networks for the future smart systems, such as smart cities, smart grid, and smart water grid. His research interests include wireless sensor and actuator networks, low-power wide area networks, software defined wireless sensor networks, cognitive radio, network security, network management, and sensor/actuator node development. He is a member of the many IEEE technical communities. He is an Associate Editor of IEEE ACCESS, IEEE INTERNET OF THINGS, and IEEE TRANSACTION ON INDUSTRIAL INFORMATICS.

LING CHENG (Senior Member, IEEE) received the B. Eng. degree from Huazhong University of Science and Technology, in 1995, and the M. Ing. and D. Ing. degrees from the University of Johannesburg, in 2005 and 2011, respectively. He is currently a Full Professor with the University of the Witwatersrand, Johannesburg, South Africa. He has published over 100 papers in journals and conference proceedings. His research interests include telecommunications and artificial intelligence. He is the Vice-Chair of the IEEE South African Information Theory Chapter.